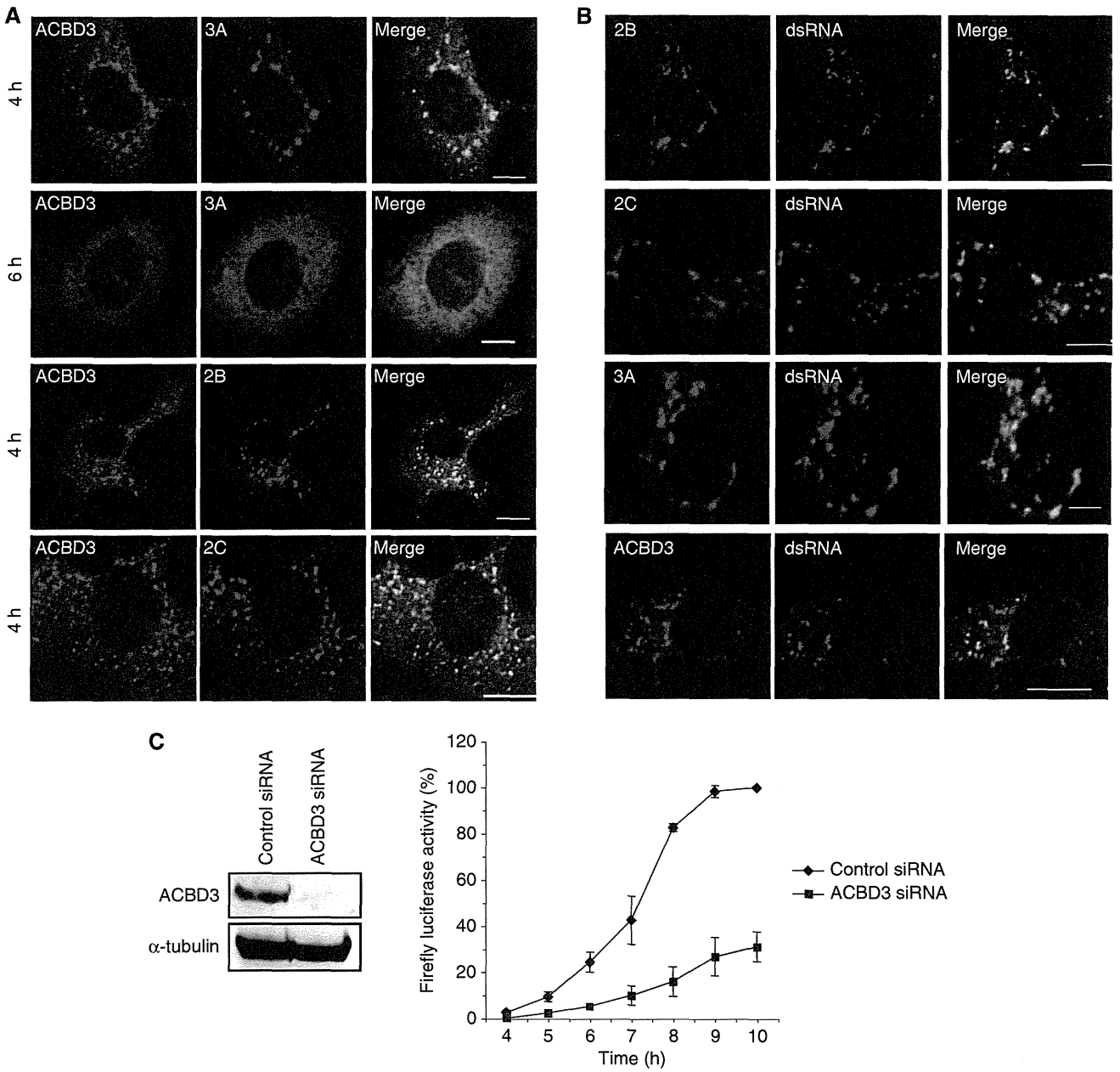

Figure 3 (**A**) Colocalization of ACBD3 with 2B, 2C, and 3A. Vero cells were electroporated with replicon RNA, AV-FL-Luc-5′rzm. At 4 or 6 h after electroporation, the cells were fixed and double stained with rabbit anti-ACBD3 and guinea pig anti-3A, anti-2B, or anti-2C antibodies. (**B**) Colocalization of dsRNA with ACBD3, 2B, 2C, or 3A. Vero cells were electroporated with replicon RNA. At 4 h, the cells were fixed and double stained with anti-dsRNA (mouse) and anti-2B, anti-2C, anti-3A, or anti-ACBD3 antibodies (rabbit). Bars represent 30 μm. (**C**) Effect of knockdown of ACBD3 on AiV replication. Vero cells were transfected with 80 nM of either control siRNA or siRNA against ACBD3. At 72 h after transfection, lysates were prepared and subjected to immunoblotting to assess the levels of ACBD3 and α-tubulin (left panel). At 72 h post transfection with siRNAs, the cells were transfected with replicon RNA and then luciferase activity in cell lysates harvested at the indicated times was measured (right panel). The maximum value obtained for cells treated with control siRNA was taken as 100%. The experiment was repeated at least three times. Standard deviation bars are shown.

was almost completely inhibited at 5 μM (Figure 5A). Cell viability was not affected by treatment with 5 μM (data not shown). It is noted that at 1 h after electroporation, the level of luciferase activity observed for T-00127-HEV1-treated cells was similar to that for cells treated with DMSO, and was significantly higher than that for mock-transfected cells. At this time point, viral RNA replication does not occur, and the obtained luciferase activity mainly results from translation of input RNA (Sasaki and Taniguchi, 2008). Thus, this result suggests that PI4KB activity is important for AiV RNA replication, but not for translation.

Furthermore, we investigated viral RNA replication in PI4KB knockdown cells. Vero cells were treated with siRNA targeting PI4KB or control siRNA. At 72 h after treatment with siRNA targeting PI4KB, a decrease in the amount of PI4KB was observed (Figure 5B). Cell viability was not affected by treatment with siRNA targeting PI4KB (data not shown). At 72 h after siRNA treatment, AV-FL-Luc-5′rzm RNA was

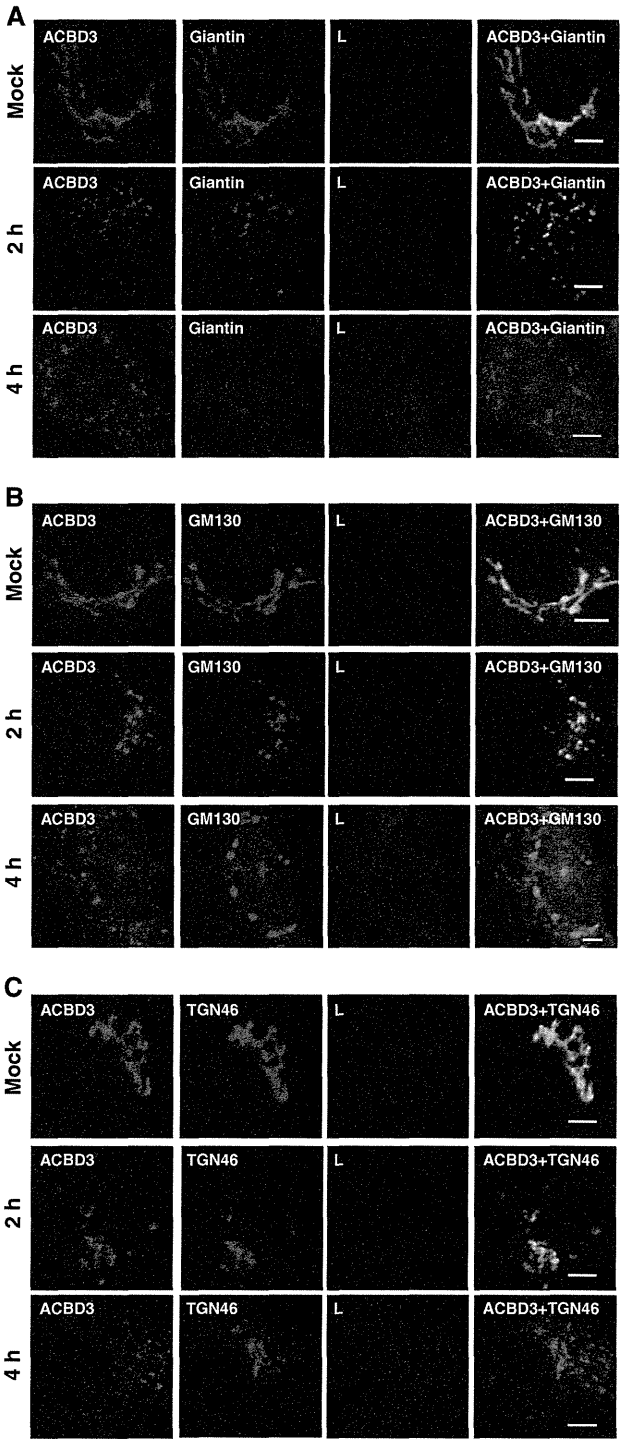

Figure 4 Dynamics of different Golgi proteins during AiV RNA replication. Vero cells were mock electroporated or electroporated with the replicon RNA, AV-FL-Luc-5′rzm. At 2 or 4 h after electroporation, the cells were fixed and triple stained with rabbit anti-ACBD3, guinea pig anti-L, and (**A**) mouse anti-giantin, (**B**) mouse anti-GM130, or (**C**) sheep anti-TGN46 antibodies. Bars represent 30 μm.

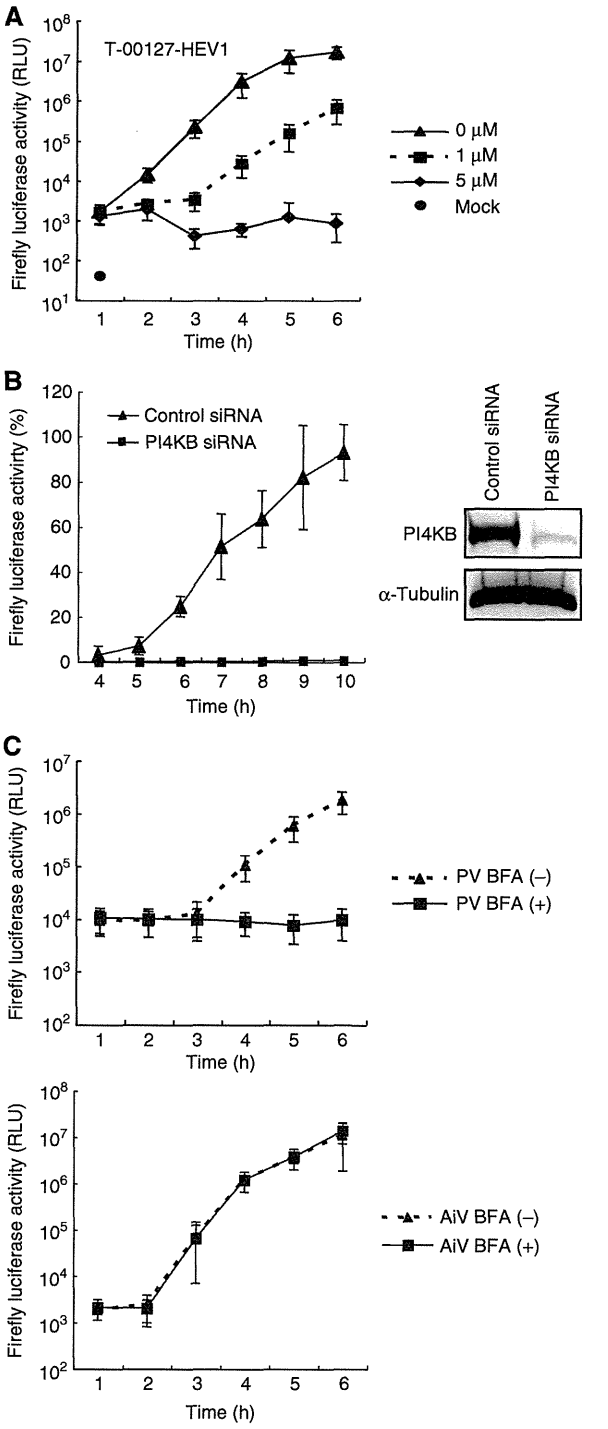

Figure 5 (**A**) T-00127-HEV1 inhibits AiV RNA replication. Vero cells were mock electroporated or electroporated with the replicon RNA, AV-FL-Luc-5′rzm, and then treated with 0 (DMSO), 1 or 5 μM T-00127-HEV1. After incubation for the indicated times, the cells were assayed for luciferase activity. (**B**) Depletion of endogenous PI4KB severely reduces AiV RNA replication. Vero cells were transfected with 40 nM control siRNA or siRNA against PI4KB. At 72 h after transfection, the levels of PI4KB and α-tubulin were determined by immunoblotting (right panel), and the subsequent analysis was performed as in Figure 3C (left panel). (**C**) AiV RNA replication is insensitive to BFA. Vero cells were electroporated with poliovirus (PV) (upper panel) or AiV (lower panel) replicon RNA and then incubated with or without 10 μg/ml of BFA. After incubation for the indicated times, the cells were assayed for luciferase activity. All experiments were repeated at least three times. Standard deviation bars are shown.

transfected by lipofection, and RNA replication was examined by a luciferase assay. Knockdown of PI4KB almost completely inhibited AiV RNA replication, and at 10 h after transfection, luciferase activity was decreased by 99% (Figure 5B). A similar result was obtained using HeLa cells (data not

shown). These results indicate that PI4KB activity is essential for AiV RNA replication.

PI4KB interacts with ACBD3

BFA is an inhibitor of enterovirus RNA replication (Irurzun *et al*, 1992; Maynell *et al*, 1992). BFA inactivates GBF1 (Peyroche *et al*, 1999) and inhibits recruitment of GBF1/Arf1 to 3A, resulting in inhibition of recruitment of PI4KB to the replication sites of enteroviruses (Belov *et al*, 2008; Hsu *et al*, 2010). We investigated whether BFA inhibits AiV replication. Treatment with 10 μg/ml of BFA inhibited poliovirus RNA replication, as known, but did not affect AiV RNA replication at all (Figure 5C). This result suggests that PI4KB is recruited independently of GBF1/Arf1 to the AiV replication sites. As described above, ACBD3 was localized to the Aichi viral RNA replication sites through binding to some viral non-structural proteins. We examined whether ACBD3 interacts with PI4KB. In the mammalian two-hybrid assay, interaction between ACBD3 and PI4KB resulted in a 138-fold increase in luciferase activity, indicating a strong interaction between the two proteins (Figure 6A). No apparent activation of luciferase expression was detected for viral non-structural proteins (3.5-fold increase for 3A and less for other proteins). To further confirm the interaction between ACBD3 and PI4KB, HA-tagged PI4KB was co-expressed with FLAG-tagged ACBD3 or FLAG-tagged 3A in 293T cells, and then co-immunoprecipitation analysis was performed. As shown in Figure 6B, PI4KB was co-immunoprecipitated with ACBD3, but not with 3A, confirming the interaction between ACBD3 and PI4KB.

PI4KB interacts with the central part of ACBD3

To determine the PI4KB-binding domain of ACBD3, interactions of deletion mutants of ACBD3 with PI4KB were investigated in the mammalian two-hybrid system (Figure 6C). Of the five mutants shown in Figure 2A, mut2 and mut5 activated luciferase expression strongly (~15- and 45-fold, respectively), implying the importance of a wider region including aa 171–327 of ACBD3 for binding to PI4KB. Additional two mutants, mut6 and mut7, which contain aa 116–327 and aa 116–428, respectively, exhibited the ability to strongly activate luciferase expression (24- and 32-fold, respectively). These results suggest that the central part of ACBD3 (aa 116–327) is important for binding to PI4KB. In addition, the PI4KB-binding domain was suggested not to overlap with the binding domain for 2B, 2BC, 2C, 3A, and 3AB (aa 374–528).

PI4KB colocalizes with ACBD3, 2B, 2C, 3A, and dsRNA in AiV RNA-transfected cells

We examined whether PI4KB localizes to the viral RNA replication sites. In mock-transfected cells, PI4KB mainly localized to the Golgi, and colocalized with ACBD3 (Figure 7A). When ACBD3 expression was knockdown by using siRNA, PI4KB was dispersed in the cytoplasm and did not localize to the Golgi (Figure 7B), strongly suggesting a critical role of ACBD3 in Golgi recruitment of PI4KB. In viral RNA-replicating cells, PI4KB colocalized with ACBD3, 2B, 2C, 3A, and dsRNA (Figure 7A and C). Treatment of mock-transfected cells with BFA resulted in dispersion of ACBD3 and PI4KB to the cytoplasm (Figure 7D). In contrast, in viral RNA-transfected cells with BFA treatment, ACBD3 and PI4KB

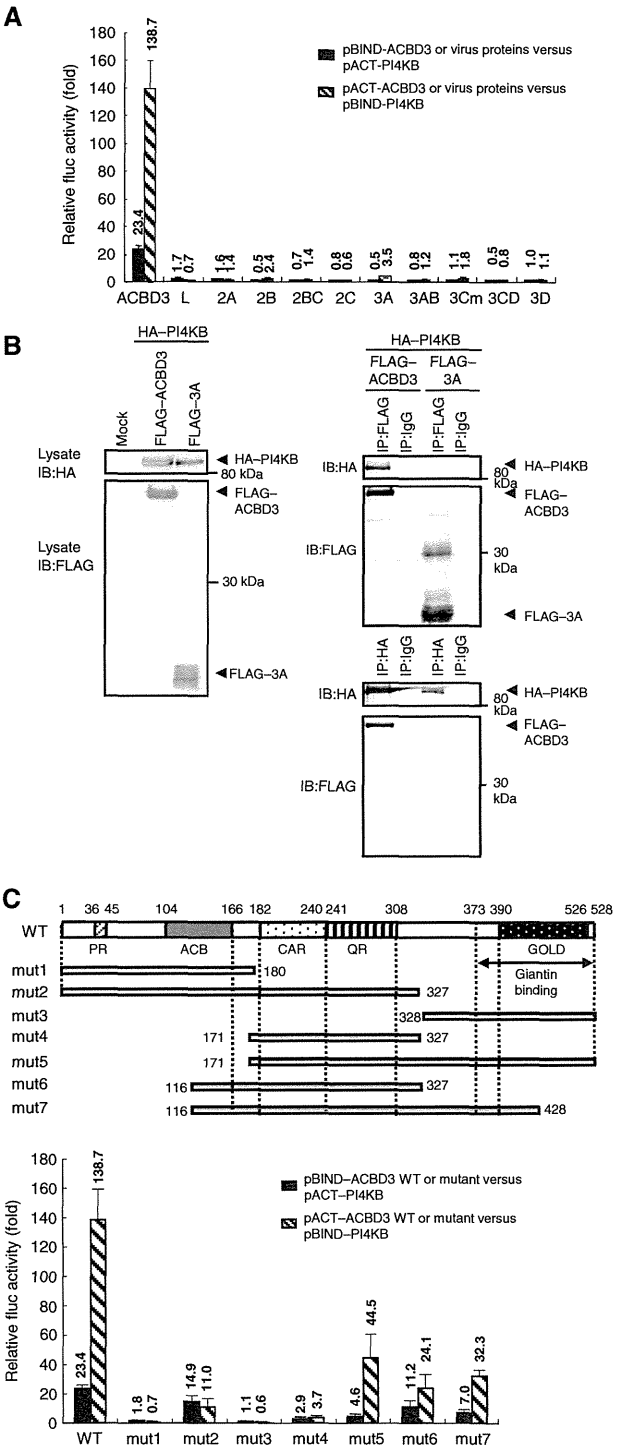

Figure 6 PI4KB interacts with ACBD3. (**A**) The mammalian two-hybrid assay was performed to examine interactions between PI4KB and ACBD3 or the virus proteins and the results are represented as in Figure 1A. (**B**) Co-immunoprecipitation of PI4KB with ACBD3. HA-tagged PI4KB was co-expressed with FLAG-tagged ACBD3 or FLAG-tagged 3A in 293T cells, and the subsequent analysis was performed as in Figure 1B. (**C**) Mapping of the PI4KB-binding region of ACBD3. Schematic representation of full-length ACBD3 (WT) and its mutants (mut6 and mut7) (upper panel). Mammalian two-hybrid analysis was performed to examine interactions between PI4KB and ACBD3 WT or its mutants (mut1–7), and the results are represented as described in Figure 1A (lower panel). Figure source data can be found in Supplementary data.

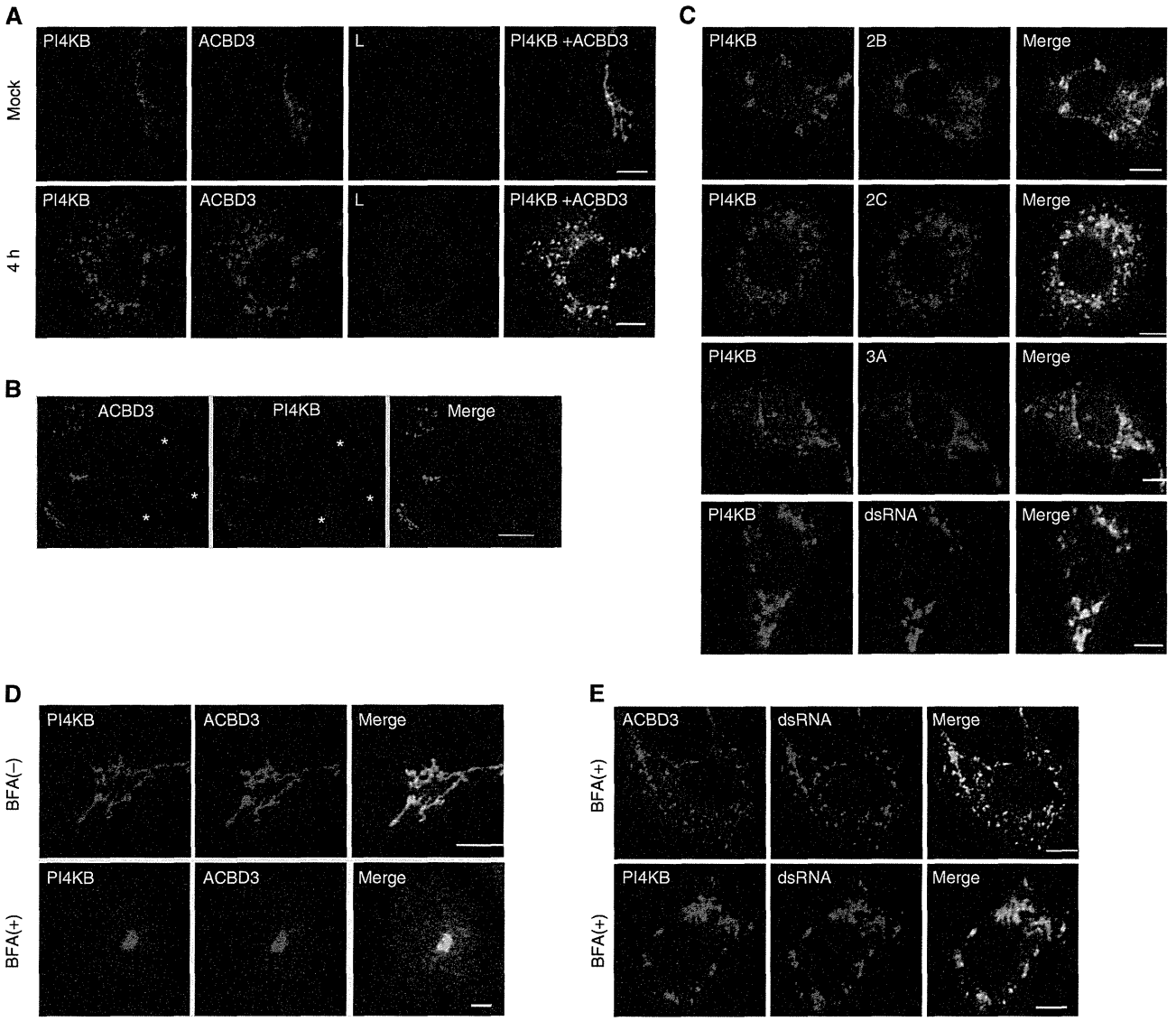

Figure 7 PI4KB is recruited to the AiV RNA replication sites through interaction with ACBD3 associated with the viral proteins. (**A**) Colocalization of PI4KB with ACBD3. Vero cells were mock electroporated or electroporated with the replicon RNA, AV-FL-Luc-5′rzm. At 4 h after electroporation, the cells were fixed and triple stained with mouse anti-PI4KB, rabbit anti-ACBD3, and guinea pig anti-L antibodies. (**B**) Effect of ACBD3 knockdown on the localization of PI4KB. Vero cells were transfected with siRNA against ACBD3. At 72 h after transfection, cells were fixed and double stained with anti-ACBD3 and anti-PI4KB. Asterisks indicate cells where knockdown of the expression of ACBD3 was observed. (**C**) PI4KB colocalizes with 2B, 2C, 3A, or dsRNA. At 4 h after electroporation with the replicon RNA, the Vero cells were fixed and double stained with mouse anti-PI4KB and rabbit anti-2B, -2C, or -3A antibodies, or rabbit anti-PI4KB and mouse anti-dsRNA antibodies. (**D**, **E**) Recruitment of PI4KB and ACBD3 to the AiV RNA replication sites is not affected by BFA. Vero cells were (**D**) mock electroporated or (**E**) electroporated with the replicon RNA, and then incubated in medium with or without 10 μg/ml of BFA. At 4 h after electroporation, the cells were fixed and immunostained with the indicated antibodies. Bars represent 30 μm.

formed clusters in the cytoplasm, and colocalized with dsRNA (Figure 7E). These results indicate that PI4KB is present in the viral RNA replication sites through interaction with ACBD3, which is recruited through interaction with 2B, 2BC, 2C, 3A, and 3AB. In addition, it was shown that recruitment of PI4KB and ACBD3 to the AiV RNA replication sites was not affected by BFA.

PI4P accumulates in viral RNA replication sites

We examined whether recruitment of PI4KB to the sites for AiV RNA replication results in accumulation of PI4P. In mock-transfected cells, PI4P mainly localized to the Golgi, and colocalized with ACBD3 and PI4KB (Figure 8A). In viral RNA-replicating cells, PI4P formed clusters in the cytoplasm, and colocalized with ACBD3, PI4KB, 2B, 2C, 3A, and dsRNA (Figure 8A and B). These results indicate that PI4P accumulates in AiV RNA replication sites.

Discussion

AiV is a member of the family *Picornaviridae*, and belongs to a different genus from the well-characterized picornaviruses, enteroviruses such as poliovirus and CVB3. In this study, we showed that AiV non-structural proteins and cleavage intermediates, 2B, 2BC, 2C, 3A, and 3AB, interact with ACBD3. Furthermore, ACBD3 was shown to interact with PI4KB.

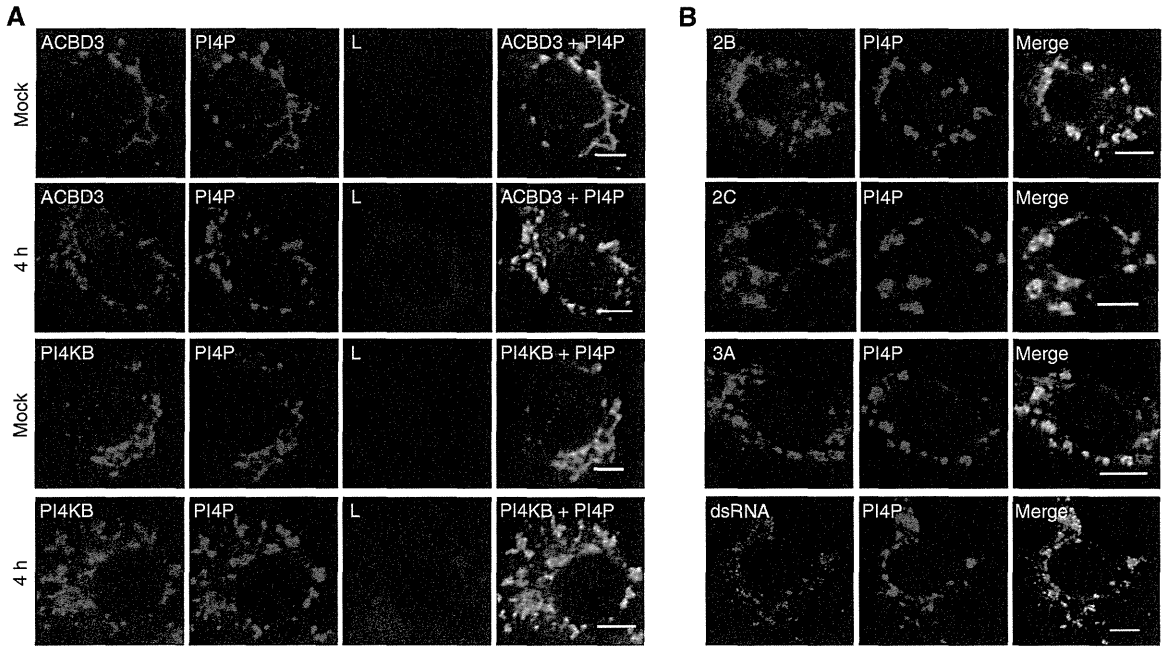

Figure 8 PI4P localizes to the AiV RNA replication sites. (**A**, **B**) Vero cells were electroporated with mock or replicon RNA. At 4 h after electroporation, the cells were fixed and immunostained with the indicated antibodies. Bars represent 30 μm.

Immunofluorescence microscopy showed that dsRNA, which indicates the viral RNA replication sites, colocalized with these viral proteins, ACBD3, PI4KB, and PI4P lipids. In addition, knockdown of ACBD3 or PI4KB using siRNA inhibited AiV RNA replication. These results indicate that the viral protein/ACBD3/PI4KB complex is formed to synthesize PI4P at the viral RNA replication sites and plays an essential role in viral RNA replication.

PI4KB has been reported to be an essential host factor for enterovirus RNA replication (Hsu *et al*, 2010; Arita *et al*, 2011). According to the model proposed by Hsu *et al* (2010), PI4KB is recruited to the RNA replication sites by GBF1/Arf1/3A, and synthesizes PI4P. PI4P can interact with viral RNA polymerase 3D, a soluble protein. Thus, soluble 3D is recruited to the viral RNA replication complex formed on membranes to facilitate viral RNA synthesis. BFA inactivates GBF1 and inhibits the recruitment of GBF1/Arf1 to 3A, thereby inhibiting recruitment of PI4KB to the replication sites of enteroviruses (Belov *et al*, 2008; Hsu *et al*, 2010). The present study showed that AiV replication was insensitive to BFA (Figure 5C). The difference in the sensitivity to BFA between AiV and enteroviruses can be explained by the difference in the strategy used to recruit PI4KB to the viral RNA replication sites. In AiV, PI4KB would be recruited to the viral RNA replication sites through the formation of the viral protein/ACBD3/PI4KB complex. Formation of this complex would be resistant to BFA, as indicated by the observation that PI4KB as well as ACBD3 colocalized with dsRNA even in the presence of BFA (Figure 7E). This result is in contrast to the observation that PI4KB disperses in BFA-treated CVB3-infected cells (Hsu *et al*, 2010). It remains to be determined whether PI4P can bind to AiV 3D RNA polymerase.

It is known that PI4KB is recruited to the Golgi by Arf1 (Godi *et al*, 1999). The present study would be the first report that PI4KB interacts with ACBD3. Knockdown of ACBD3 resulted in abrogation of Golgi localization of PI4KB (Figure 7B), suggesting a critical role of ACBD3 in Golgi recruitment of PI4KB. ACBD3 is also known as peripheral-type benzodiazepine receptor and cAMP-dependent protein kinase-associated protein 7 (PAP7) (Li *et al*, 2001) or Golgi complex-associated protein of 60 kDa (GCP60) (Sohda *et al*, 2001). ACBD3 is localized to the Golgi and also to mitochondria (Li *et al*, 2001; Sohda *et al*, 2001), and has various biological functions (reviewed in Fan *et al*, 2010) in the maintenance of the Golgi apparatus structure (Sohda *et al*, 2001), apoptosis (Sbodio *et al*, 2006), steroidogenesis (Li *et al*, 2001), neurogenesis (Cheah *et al*, 2006), and embryogenesis (Zhou *et al*, 2007). Studies to elucidate the biological significance of the interaction between ACBD3 and PI4KB will help to further understand the biological functions of these proteins.

ACBD3 contains no hydrophobic region that can be involved in membrane localization, and is localized to the Golgi through interaction with giantin, which contains a C-terminal membrane-anchoring domain (Sohda *et al*, 1994, 2001). The giantin-binding domain of ACBD3 has been mapped to the C-terminal region (aa 373–528). Our mammalian two-hybrid assays indicated that the giantin-binding domain of ACBD3 overlapped with the binding domain for the five viral nonstructural proteins (aa 374–528) (Figure 2), but did not overlap with the PI4KB-binding domain, which was mapped to the central region (aa 116–327) (Figure 6C). This implies that PI4KB is at least partly present in the Golgi through interaction with the ACBD3/giantin complex. We propose a model for recruitment of PI4KB to the AiV RNA replication sites (Figure 9). The viral membrane proteins 2B, 2BC, 2C, 3A, and 3AB will compete with giantin for binding to ACBD3 at the Golgi. As infection progresses, the viral proteins will rob the preexisting giantin/ACBD3/PI4KB complex of the ACBD3/PI4KB complex to form the viral protein/ACBD3/PI4KB complex. This is also suggested by the subcellular localization of these proteins shown in Figures 3, 4A, and 7.

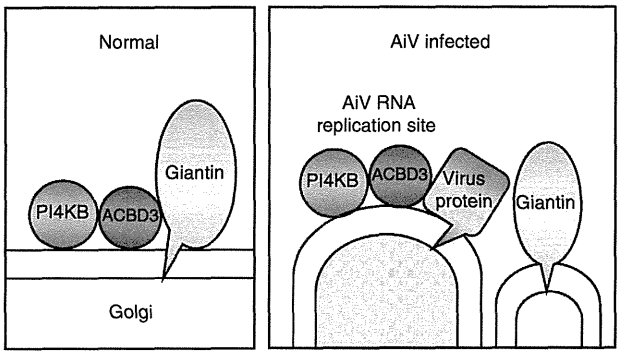

Figure 9 Model for recruitment of PI4KB to the AiV replication sites. In uninfected cells, the C-terminal region of ACBD3 binds to the C-terminal cytoplasmic domain of giantin that is anchored to the Golgi membrane through the C-terminal anchoring domain. PI4KB is localized to the Golgi through interaction with the central part of ACBD3 (left panel). In AiV-infected cells, viral membrane proteins 2B, 2BC, 2C, 3A, and 3AB compete with giantin at the Golgi for binding to ACBD3. The viral protein/ACBD3/PI4KB complex is formed as infection progresses, whereas giantin no longer colocalizes with ACBD3 (right panel).

ACBD3 targeting of the multiple viral proteins may result in increases in the concentrations of the viral proteins at the Golgi to facilitate formation of viral replication complexes. In addition, binding of multiple viral proteins to ACBD3 that has the ability to associate with PI4KB would lead to efficient recruitment of PI4KB to the viral RNA replication sites.

The redistribution of giantin, GM130, and TGN46 to the cytoplasm observed in AiV-replicating cells (Figure 4) indicates Golgi disassembly. It has been reported that ACBD3 is involved in the maintenance of the Golgi structure by interacting with giantin (Sohda *et al*, 2001). Dissociation of ACBD3 from giantin through bound by the viral proteins may contribute to Golgi disassembly. At 4 h after electroporation with the replicon RNA, 2B, 2C, and 3A colocalized with ACBD3 in patchy structures in the cytoplasm (Figure 3A). On the other hand, giantin, GM130, and TGN46 redistributed to the cytoplasm did not colocalize with ACBD3 (Figure 4). Considering that the virus membrane proteins 2B, 2C, and 3A target ACBD3, it is very likely that these viral proteins are first accumulated in the Golgi, and then the replication complexes are formed utilizing Golgi membranes; however, the mechanism of the membrane remodelling for formation of the AiV replication complexes is currently unknown. Interestingly, acyl-coenzyme A (acyl-CoA) has been reported to participate in the budding of transport vesicles from Golgi cisternae and the fusion of transport vesicles with Golgi cisternae (Glick and Rothman, 1987; Pfanner *et al*, 1989, 1990). ACBD3-bound acyl-CoA may play a role in membrane remodelling for formation of the viral RNA replication complexes. In addition, the absence of three Golgi proteins, giantin, GM130, and TGN46, at the AiV RNA replication sites suggests the sorting or deterring of Golgi components, which has been observed in CVB3-infected cells (Hsu *et al*, 2010). TGN46 is present at the sites for CVB3 replication, but was absent at the AiV replication sites. On the other hand, the absence of GM130 was observed in the replication sites for the two viruses. These imply a different manner of sorting or deterring of the Golgi components between AiV and CVB3. Analysis of the subcellular localization of other Golgi components and factors involved in intracellular membrane traffic in AiV-infected cells will be required for elucidation of the mechanism of formation of the AiV replication complexes.

The C-terminal region of ACBD3 interacting with the AiV proteins as well as giantin is known as the GOLD (Golgi dynamics) domain (Figure 2A). The GOLD domain is typically 90–150 aa long and folds into six or seven β-strands. This domain has been identified in several proteins with roles in Golgi dynamics and secretion including p24 proteins and Sec14 proteins, and is thought to serve as a common denominator in protein–protein interactions (Anantharaman and Aravind, 2002). It would be interesting to investigate whether the AiV proteins have the ability to bind to other GOLD domain-containing proteins.

In conclusion, the present study demonstrated that AiV utilized a different strategy to recruit PI4KB to the replication sites from enteroviruses, that is, through viral protein/ACBD3/PI4KB interactions. ACBD3-mediated recruitment of PI4KB to the replication sites was resistant to BFA. The sensitivity of viral replication to BFA varies among different picornaviruses. HAV is sensitive and human parechovirus is partly sensitive. On the other hand, FMDV and encephalomyocarditis virus are insensitive (Blank *et al*, 2000; Gazina *et al*, 2002; Monaghan *et al*, 2004). It would be of interest to investigate whether all picornaviruses require PI4KB for replication and, if so, how PI4KB is recruited to the replication sites.

Materials and methods

Cell lines and reagents

Vero (African green monkey kidney cell line) and 293T (human embryonic kidney cell line) cells were maintained in Eagle's minimum essential medium supplemented with 5 and 10% fetal bovine serum, respectively, at 37°C. BFA was purchased from Sigma, and diluted in ethanol. T-00127-HEV1 was described previously (Arita *et al*, 2011), and diluted in DMSO.

Replicon RNAs of AiV and poliovirus

The AiV and poliovirus replicon RNAs containing a firefly luciferase gene (AV-FL-Luc-5′rzm RNA and PV-Fluc mc RNA, respectively) were generated by *in-vitro* transcription using a T7 RiboMAX express large scale RNA production system (Promega) from *Hin*dIII-linearized pAV-FL-Luc-5′rzm (Sasaki and Taniguchi, 2003; Nagashima *et al*, 2005) and *Dra*I-linearized pPV-Fluc mc (Arita *et al*, 2006), respectively. Lysates of cells transfected with the replicon RNAs were prepared using a Passive lysis buffer (Promega) and subjected to a luciferase assay using a Luciferase assay system (Promega) and a luminometer, Lumat LB9507 (Berthold).

Plasmids

The construction of pBIND-L, -2A, -2B, -2BC, -2C, -3A, -3AB, -3Cm, -3CD, and -3D, and pACT-L, -2A, -2B, -2BC, -2C, -3A, -3AB, -3Cm, -3CD, and -3D was described previously (Ishikawa *et al*, 2010). The coding region of ACBD3 was amplified by PCR from a cDNA clone (Toyobo, FCC137B01), while the PI4KB-coding sequence was amplified by RT–PCR using total RNA prepared from HeLa cells. Each PCR product was cloned into pBIND and pACT (Promega) as described previously (Ishikawa *et al*, 2010), yielding pBIND-ACBD3 and -PI4KB, and pACT-ACBD3 and -PI4KB. pBIND and pACT constructs encoding ACBD3 deletion mutants (pBIND- or pACT-ACBD3-mut1, -mut2, -mut3, -mut4, -mut5, -mut6, -mut7, -mut3Δ1, -mut3Δ2, -mut3Δ3, -mut3Δ4, and -mut3Δ5) were generated by cloning each DNA fragment amplified by PCR from pACT-ACBD3 into pBIND and pACT. The DNA fragments encoding L, 2B, 2BC, 2C, 3A, and 3AB were obtained by PCR from pAV-FL-Luc-5′rzm. The PCR-amplified DNA fragment encoding L, 2B, 2BC, 2C, 3A, 3AB, PI4KB, or ACBD3 was cloned into pCI mammalian expression vector (Promega) containing an HA or FLAG tag-coding sequence to

produce an N-terminally HA- or FLAG-tagged protein (pCI-HA-L, pCI-HA-2B, pCI-HA-2BC, pCI-HA-2C, pCI-HA-3A, pCI-HA-3AB, and pCI-HA-PI4KB, and pCI-FLAG-3A and pCI-FLAG-ACBD3). To construct bait plasmids for the yeast two-hybrid assays, the 2B-, 2C- and 3A-coding regions were amplified by PCR and then cloned into pGBKT7 (Clontech), resulting in pGBKT7-2B, -2C, and -3A. The nucleotide sequences of all the PCR products were verified. For expressing MBP-fused 2B, 2C, or 3A in *E. coli*, these genes were amplified by PCR and cloned into pMAL-c2X (New England Biolabs). pMAL-3AB was described previously (Nagashima *et al*, 2008). For expressing GST-fused ACBD3, PCR-amplified ACBD3-coding sequence was cloned into pGEX-6P3 (Amersham Pharmacia Biotech).

Antibodies

Rabbit or guinea pig polyclonal antibody to 3A was obtained by immunization with the His-tagged 3A protein expressed in *Escherichia coli*. Rabbit or guinea pig polyclonal antibodies to 2B and 2C were obtained by immunization with a mixture of two peptides (2B: GLLTLSADTETNQTLNKC and SQFDLSGPANSV-SLAASC; and 2C: CPFDPTNALNPIPGTQSK and IRGKAKTDPQAK-LADVHC). The preparation of guinea pig polyclonal antibody to L was described previously (Sasaki *et al*, 2003). Mouse monoclonal antibodies to HA tag, FLAG tag, ACBD3 (clone G2G), and α-tubulin, and rabbit polyclonal antibodies to FLAG tag and ACBD3 were purchased from Sigma; mouse monoclonal antibody to GST from Wako; rabbit polyclonal antibody to HA tag from Bethyl; rabbit polyclonal antibody to PI4KB from Millipore; mouse monoclonal antibodies to GM130 and PI4KB from BD Biosciences; mouse monoclonal antibody to giantin from Abcam; sheep polyclonal antibody to TGN46 was from AbD serotec; anti-PI4P antibody (mouse monoclonal IgM) from Echelon Biosciences; mouse monoclonal antibody to dsRNA (clone J2) from English and Scientific Consulting; Alexa Fluor 488-conjugated anti-mouse IgG and anti-rabbit IgG antibodies, Alexa Fluor 594-conjugated anti-mouse IgG, anti-mouse IgM, anti-rabbit IgG, anti-sheep IgG, and anti-guinea pig IgG antibodies from Molecular Probes; AMCA-conjugated anti-guinea pig IgG from Millipore; and horseradish peroxidase (HRP)-conjugated antibodies from Zymed.

Yeast two-hybrid assays

Yeast two-hybrid assays were performed with a Matchmaker two-hybrid system 3 (Clontech) according to the manufacturer's instructions. The bait plasmid encoding 2B, 2C or 3A, pGBKT-2B, -2C or -3A, was transformed into *Saccharomyces cerevisiae* strain AH109, and the individual transformants were mated with *S. cerevisiae* strain Y187 pretransformed with a human HeLa cDNA library (Clontech) constructed in pGADT7. The resulting diploids were screened on agar plates of dropout medium lacking adenine, histidine, leucine, and tryptophan, supplemented with X-alpha-Gal (5-bromo-4-chloro-3-indolyl-alpha-*O*-galactopyranoside). The insert DNAs of yeast clones grown on plates were amplified by PCR and sequenced directly.

Mammalian two-hybrid assays

The mammalian two-hybrid assays were performed as described previously using a Checkmate mammalian two-hybrid system (Promega) (Ishikawa *et al*, 2010). The ability of viral protein gene-containing constructs to express fusion proteins was examined previously (Ishikawa *et al*, 2010). Expression of the ACBD3 constructs and deletion mutants were also examined by immunoblotting as described previously (Ishikawa *et al*, 2010) and confirmed expression of fusion proteins for mutants that exhibited no increase in luciferase activity (data not shown).

DNA transfection, immunoprecipitation, and immunoblotting

Transfection of plasmid DNA was carried out using a FuGENE HD transfection reagent (Roche) according to the manufacturer's protocol. For the immunoprecipitation assays, 293T cells were grown in 6-well plates for 24 h and then transfected with HA- and FLAG-tagged constructs (2 μg/well). At 24 h (for co-expression of HA-2B, HA-2C, HA-3A, or HA-PI4KB) or 48 h (for co-expression of HA-2BC or HA-3AB) after transfection, cells were washed three times with phosphate-buffered saline (PBS) and then lysed in 350 μl lysis buffer (50 mM Tris-HCl, pH 8.0, 150 mM NaCl, 1% or 0.2% Nonidet P-40 (NP-40), 1 mM phenylmethylsulphonyl fluoride) supplemented with a protease inhibitor cocktail and a phosphatase inhibitor cocktail (Sigma). Cell lysates were centrifuged at 12 000 *g* for 10 min, and the supernatants were immunoprecipitated with 50 μl of Dynabeads Protein G (Dynal) coated with 1 μg of antibody at 4°C for 1 h. After washing three times with lysis buffer and then one time with wash buffer (50 mM Tris-HCl pH 8.0), the beads were boiled in SDS-PAGE sample buffer. The immunoprecipitates were separated by 12.5% or 7.5% SDS-PAGE and then transferred onto polyvinylidene difluoride membranes (Bio-Rad). The membranes were probed with appropriate primary antibodies, followed by incubation with HRP-conjugated secondary antibodies. The chemiluminescence signals were visualized using ECL Advance reagents (Amersham Biosciences) and an LAS-4000UVmini (Fujifilm).

MBP pull-down assay

MBP, MBP-2B, MBP-2C, MBP-3A, and MBP-3AB, and GST-ACBD3 were expressed in *E. coli* BL21 cells according to the manufacturer's protocols. For purifying GST-ACBD3, harvested cells were suspended in Buffer A (140 mM NaCl, 2.7 mM KCl, 10 mM Na_2HPO_4, 1.8 mM KH_2PO_4, pH 7.4) and lysed by sonication. The lysate was mixed with 50% glutathione-Sepharose slurry (GE Healthcare) and incubated for 4 h at 4°C. After the beads were washed three times with Buffer A, GST-ACBD3 were eluted with elution buffer (50 mM Tris-HCl, 10 mM reduced glutathione, pH 8.0). Cells expressing MBP or MBP-fused viral proteins were suspended in Column buffer (20 mM Tris-HCl, 200 mM NaCl, 1 mM EDTA, pH 7.5) and lysed by sonication, and the lysates were incubated with 7.5 μl of 50% amylose resin slurry (New England Biolabs) for 90 min at 4°C. Then, the resin was washed three times with Column buffer, resuspended in NP-40 buffer (50 mM Tris-HCl, 150 mM NaCl, 1% NP-40, pH 8.0), and then mixed with purified GST-ACBD3. After incubation for 90 min at 4°C, the resin was washed five times with NP-40 buffer. Proteins binding to the resin were eluted with Column buffer containing 10 mM maltose, and analysed by SDS-PAGE, followed by immunoblotting with anti-GST antibody and Coomassie brilliant blue (CBB) staining.

Electroporation and immunofluorescence microscopy

Electroporation was performed as described previously (Sasaki *et al*, 2001). Vero cells mock electroporated or electroporated with replicon RNA were cultured on slide glasses. For BFA treatment, the electroporated cells were cultured in medium containing 10 μg/ml of BFA for 4 h. At appropriate times after electroporation, the cells were fixed with PBS containing 4% paraformaldehyde for 45 min and then permeabilized with PBS containing 0.5% Triton X-100 for 15 min or PBS containing 20 μM digitonin for 5 min only for staining PI4P. The cells were incubated with appropriate primary antibodies and then with appropriate secondary antibodies diluted in PBS containing 3% bovine serum albumin or can get signal immunostain solution A (Toyobo). The slide glasses were mounted with Fluoromount Plus (Diagnostic BioSystems) and then viewed under a fluorescence microscope, BZ-8000 (Keyence).

Gene silencing with siRNA

Control siRNA (ON-TARGET plus non-targeting siRNA#1), and siRNAs against ACBD3 and PI4KB (ON-TARGET plus SMART pool siRNA) were purchased from Dharmacon. The target sequences for ACBD3 and PI4KB were as follows: 5′-GGAUGCAGAUUCCGUGAUU-3′ (ACBD3 siRNA1), 5′-GCAACUGUACCAAGUAAUA-3′ (ACBD3 siRNA2), 5′-GCAUAUGGGAAGUAACAUU-3′ (ACBD3 siRNA3), 5′-GUAUAGAAACCAUGGAGUU-3′ (ACBD3 siRNA4), 5′-CCUUUAAGC UGACCACAGA-3′ (PI4KB siRNA1), 5′-CCGAGAGUAUUGAUAAUUC-3′ (PI4KB siRNA2), 5′-CCCAGUUGCUUAACAUGUA-3′ (PI4KB siRNA3), and 5′-GGACUCACCAGCGCUCUAA-3′ (PI4KB siRNA4). A mixture of these four siRNAs was used for gene silencing of ACBD3 or PI4KB. Vero cells grown on a 48-well plate were transfected with 40 or 80 nM of siRNA using Lipofectamine RNAiMAX (Invitrogen) according to the manufacturer's protocol. The transfected cells were grown for 72 h and subjected to the following analyses. The levels of ACBD3 and PI4KB expression were evaluated by immunoblotting. Cell viability was measured using a Calcein AM Cell Viability Kit (Trevigen) according to the manufacture's protocol and calcein fluorescence was detected using a 2030 ARVO X multilabel plate reader (Perkin-Elmer). Transfection of siRNA-treated cells with the replicon RNA for the luciferase assay was performed by using Lipofectin reagent (Invitrogen) as described previously (Sasaki *et al*, 2001).

Acknowledgements

This study was supported in part by Grant-in-Aid for Scientific Research (C), and Grant-in-Aid for Scientific Research on Priority Areas: Matrix of Infection Phenomena from the Ministry of Education, Culture, Sports, Science and Technology, and Grant-in-Aid from the Ministry of Health, Labor and Welfare, Japan.

Author contributions: JS designed the experiments, performed experiments shown in Figure 1C, 5A and C, and wrote the manuscript. KI performed most of the experiments, analysed the results, and wrote the manuscript. MA contributed with important reagents and discussed the data. KT coordinated the study and oversaw the research.

Conflict of interest

The authors declare that they have no conflict of interest.

References

Aldabe R, Barco A, Carrasco L (1996) Membrane permeabilization by poliovirus proteins 2B and 2BC. *J Biol Chem* **271:** 23134–23137

Ambert-Balay K, Lorro M, Bon F, Giraudon H, Kaplon J, Wolfer M, Lebon P, Gendrel D, Pothier P (2008) Prevalence and genetic diversity of Aichi virus in community and hospitalized patients. *J Clin Microbiol* **46:** 1252–1258

Anantharaman V, Aravind L (2002) The GOLD domain, a novel protein module involved in Golgi function and secretion. *Genome Biol* **3:** research0023

Arita M, Kojima H, Nagano T, Okabe T, Wakita T, Shimizu H (2011) Phosphatidylinositol 4-kinase III beta is a target of enviroxime-like compounds for antipoliovirus activity. *J Virol* **85:** 2364–2372

Arita M, Nagata N, Sata T, Miyamura T, Shimizu H (2006) Quantitative analysis of poliomyelitis-like paralysis in mice induced by a poliovirus replicon. *J Gen Virol* **87:** 3317–3327

Belov GA, Altan-Bonnet N, Kovtunovych G, Jackson CL, Lippincott-Schwartz J, Ehrenfeld E (2007) Hijacking components of the cellular secretory pathway for replication of poliovirus RNA. *J Virol* **81:** 558–567

Belov GA, Feng Q, Nikovics K, Jackson CL, Ehrenfeld E (2008) A critical role of a cellular membrane traffic protein in poliovirus RNA replication. *PLoS Pathog* **4:** e1000216

Belov GA, Fogg MH, Ehrenfeld E (2005) Poliovirus proteins induce membrane association of GTPase ADP-ribosylation factor. *J Virol* **79:** 7207–7721

Berger KL, Cooper JD, Heaton NS, Yoon R, Oakland TE, Jordan TX, Mateu G, Grakoui A, Randall G (2009) Roles for endocytic trafficking and phosphatidylinositol 4-kinase III alpha in hepatitis C virus replication. *Proc Natl Acad Sci USA* **106:** 7577–7582

Blank CA, Anderson DA, Beard M, Lemon SM (2000) Infection of polarized cultures of human intestinal epithelial cells with hepatitis A virus: vectorial release of progeny virions through apical cellular membranes. *J Virol* **74:** 6476–6484

Cheah JH, Kim SF, Hester LD, Clancy KW, Patterson III SE, Papadopoulos V, Snyder SH (2006) NMDA receptor-nitric oxide transmission mediates neuronal iron homeostasis via the GTPase Dexras1. *Neuron* **51:** 431–440

Cho MW, Teterina N, Egger D, Bienz K, Ehrenfeld E (1994) Membrane rearrangement and vesicle induction by recombinant poliovirus 2C and 2BC in human cells. *Virology* **202:** 129–145

DeWitte-Orr SJ, Mehta DR, Collins SE, Suthar MS, Gale Jr M, Mossman KL (2009) Long double-stranded RNA induces an antiviral response independent of IFN regulatory factor 3, IFN-β promoter stimulator 1, and IFN. *J Immunol* **183:** 6545–6553

Egger D, Teterina N, Ehrenfeld E, Bienz K (2000) Formation of the poliovirus replication complex requires coupled viral translation, vesicle production, and viral RNA synthesis. *J Virol* **74:** 6570–6580

Fan J, Liu J, Culty M, Papadopoulos V (2010) Acyl-coenzyme A binding domain containing 3 (ACBD3; PAP7; GCP60): An emerging signaling molecule. *Prog Lipid Res* **49:** 218–234

Gazina EV, Mackenzie JM, Gorrell RJ, Anderson DA (2002) Differential requirements for COPI coats in formation of replication complexes among three genera of *Picornaviridae*. *J Virol* **76:** 11113–11122

Glick BS, Rothman JE (1987) Possible role for fatty acyl-coenzyme A in intracellular protein transport. *Nature* **326:** 309–312

Godi A, Pertile P, Meyers R, Marra P, Di Tullio G, Iurisci C, Luini A, Corda D, De Matteis MA (1999) ARF mediates recruitment of PtdIns-4-OH kinase-β and stimulates synthesis of PtdIns(4,5)P_2 on the Golgi complex. *Nat Cell Biol* **1:** 280–287

Goyer M, Aho LS, Bour JB, Ambert-Balay K, Pothier P (2008) Seroprevalence distribution of Aichi virus among a French population in 2006–2007. *Arch Virol* **153:** 1171–1174

Harwood LJ, Gerber H, Sobrino F, Summerfield A, McCulloug KC (2008) Dendritic cell internalization of foot-and-mouth disease virus: influence of heparan sulfate binding on virus uptake and induction of the immune response. *J Virol* **82:** 6379–6394

Hsu NY, Ilnytska O, Belov G, Santiana M, Chen YH, Takvorian PM, Pau C, van der Schaar H, Kaushik-Basu N, Balla T, Cameron CE, Ehrenfeld E, van Kuppeveld FJM, Altan-Bonnet N (2010) Viral reorganization of the secretory pathway generates distinct organelles for RNA replication. *Cell* **141:** 799–811

Hyde JL, Sosnovtsev SV, Green KY, Wobus C, Virgin HW, Mackenzie JM (2009) Mouse norovirus replication is associated with virus-induced vesicle clusters originating from membranes derived from the secretory pathway. *J Virol* **83:** 9709–9719

Irurzun A, Perez L, Carrasco L (1992) Involvement of membrane traffic in the replication of poliovirus genomes: effects of brefeldin A. *Virology* **191:** 166–175

Ishikawa K, Sasaki J, Taniguchi K (2010) Overall linkage map of the nonstructural proteins of Aichi virus. *Virus Res* **147:** 77–84

Jackson WT, Giddings TH, Taylor MP, Mulinyawe S, Rabinovitch M, Kopito RR, Kirkegaard K. (2005) Subversion of cellular autophagosomal machinery by RNA viruses. *PLoS Biol* **3:** e156

Knoops K, Kikkert M, van den Worm SHE, Zevenhoven-Dobbe JC, van der Meer Y, Koster AJ, Mommaas AM, Snijder EJ (2008) SARS-coronavirus replication is supported by a reticulovesicular network of modified endoplasmic reticulum. *PLoS Biol* **6:** e226

Knox C, Moffat K, Ali S, Ryan M, Wileman T (2005) Foot-and-mouth disease virus replication sites form next to the nucleus and close to the Golgi apparatus, but exclude marker proteins associated with host membrane compartments. *J Gen Virol* **86:** 687–696

Krogerus C, Samuilova O, Pöyry T, Jokitalo E, Hyypiä T (2007) Intracellular localization and effects of individually expressed human parechovirus 1 non-structural proteins. *J Gen Virol* **88:** 831–841

Lanke KHW, van der Schaar HM, Belov GA, Feng Q, Duijsings D, Jackson CL, Ehrenfeld E, van Kuppeveld FJM (2009) GBF1, a guanine nucleotide exchange factor for Arf, is crucial for coxsackievirus B3 RNA replication. *J Virol* **83:** 11940–11949

Li H, Degenhardt B, Tobin D, Yao ZX, Tasken K, Papadopoulos V (2001) Identification, localization, and function in steroidogenesis of PAP7: a peripheral-type benzodiazepine receptor- and PKA (RIalpha)-associated protein. *Mol Endocrinol* **15:** 2211–2228

Maynell LA, Kirkegaard K, Klymkowsky MW (1992) Inhibition of poliovirus RNA synthesis by brefeldin A. *J Virol* **66:** 1985–1994

Miller S, Krijnse-Locker J (2008) Modification of intracellular membrane structures for virus replication. *Nat Rev Microbiol* **6:** 363–374

Miller S, Sparacio S, Bartenschlager R (2006) Subcellular localization and membrane topology of the Dengue virus type 2 nonstructural protein 4B. *J Biol Chem* **281:** 8854–8863

Moffat K, Howell G, Knox C, Belsham GJ, Monaghan P, Ryan MD, Wileman T (2005) Effects of foot-and-mouth disease virus nonstructural proteins on the structure and function of the early secretory pathway: 2BC but not 3A blocks endoplasmic reticulum-to-Golgi transport. *J Virol* **79:** 4382–4395

Monaghan P, Cook H, Jackson T, Ryan M, Wileman T (2004) The ultrastructure of the developing replication site in foot-and-mouth disease virus-infected BHK-38 cells. *J Gen Virol* **85:** 933–946

Nagashima S, Sasaki J, Taniguchi K (2005) The 5′-terminal region of the Aichi virus genome encodes *cis*-acting replication elements required for positive- and negative-strand RNA synthesis. *J Virol* **79:** 6918–6931

Nagashima S, Sasaki J, Taniguchi K (2008) Interaction between polypeptide 3ABC and the 5′-terminal structural elements of the

genome of Aichi virus: implication for negative-strand RNA synthesis. *J Virol* **82:** 6161–6171

Oh DY, Silva PA, Hauroeder B, Diedrich S, Cardoso DDP, Schreier E (2006) Molecular characterization of the first Aichi viruses isolated in Europe and in South America. *Arch Virol* **151:** 1199–1206

Peyroche A, Antonny B, Robineau S, Acker J, Cherfils J, Jackson CL (1999) Brefeldin A acts to stabilize an abortive ARF-GDP-Sec7 domain protein complex: involvement of specific residues of the Sec7 domain. *Mol Cell* **3:** 275–285

Pfanner N, Glick BS, Arden SR, Rothman JE (1990) Fatty acylation promotes fusion of transport vesicles with Golgi cisternae. *J Cell Biol* **110:** 955–961

Pfanner N, Orci L, Glick BS, Amherdt M, Arden SR, Malhotra V, Rothman JE (1989) Fatty acyl-coenzyme A is required for budding of transport vesicles from Golgi cisternae. *Cell* **59:** 95–102

Pham NTK, Khamrin P, Nguyen TA, Kanti DS, Phan TG, Okitsu S, Ushijima H (2007) Isolation and molecular characterization of Aichi viruses from fecal specimens collected in Japan, Bangladesh, Thailand, and Vietnam. *J Clin Microbiol* **45:** 2287–2288

Reuter G, Boldizsár Á, Papp G, Pankovics P (2009) Detection of Aichi virus shedding in a child with enteric and extraintestinal symptoms in Hungary. *Arch Virol* **154:** 1529–1532

Rust RC, Landmann L, Gosert R, Tang BL, Hong WJ, Hauri HP, Egger D, Bienz K (2001) Cellular COPII proteins are involved in production of the vesicles that form the poliovirus replication complex. *J Virol* **75:** 9808–9818

Sasaki J, Kusuhara Y, Maeno Y, Kobayashi N, Yamashita T, Sakae K, Takeda N, Taniguchi K (2001) Construction of an infectious cDNA clone of Aichi virus (a new member of the family *Picornaviridae*) and mutational analysis of a stem-loop structure at the 5′ end of the genome. *J Virol* **75:** 8021–8030

Sasaki J, Nagashima S, Taniguchi K (2003) Aichi virus leader protein is involved in viral RNA replication and encapsidation. *J Virol* **77:** 10799–10807

Sasaki J, Taniguchi K (2003) The 5′-end sequence of the genome of Aichi virus, a picornavirus, contains an element critical for viral RNA encapsidation. *J Virol* **77:** 3542–3578

Sasaki J, Taniguchi K (2008) Aichi virus 2A protein is involved in viral RNA replication. *J Virol* **82:** 9765–9769

Sbodio JI, Hicks SW, Simon D, Machamer CE (2006) GCP60 preferentially interacts with a caspase-generated golgin-160 fragment. *J Biol Chem* **281:** 27924–27931

Sdiri-Loulizi K, Gharbi-Khélifi H, de Rougemont A, Slaheddine C, Sakly N, Ambert-Balay K, Hassine M, Neji Guédiche M, Aouni M, Pothier P (2008) Acute infantile gastroenteritis associated with human enteric viruses in Tunisia. *J Clin Microbiol* **46:** 1349–1355

Sohda M, Misumi Y, Fujiwara T, Nishioka M, Ikehara Y (1994) Molecular cloning and sequence analysis of a human 372-kDa protein localized in the Golgi complex. *Biochem Biophys Res Commun* **205:** 1399–1408

Sohda M, Misumi Y, Yamamoto A, Yano A, Nakamura N, Ikehara Y. (2001) Identification and characterization of a novel Golgi protein, GCP60, that interacts with the integral membrane protein giantin. *J Biol Chem* **276:** 45298–45306

Suhy DA, Giddings TH, Kirkegaard K (2000) Remodeling the endoplasmic reticulum by poliovirus infection and by individual viral proteins: an autophagy-like origin for virus-induced vesicles. *J Virol* **74:** 8953–8965

Teterina NL, Gorbalenya AE, Egger D, Bienz K, Ehrenfeld E (1997) Poliovirus 2C protein determinants of membrane binding and rearrangements in mammalian cells. *J Virol* **71:** 8962–8972

Towner JS, Ho TV, Semler BL (1996) Determinants of membrane association for poliovirus protein 3AB. *J Biol Chem* **271:** 26810–26818

Wessels E, Duijsings D, Lanke KHW, van Dooren SHJ, Jackson CL, Melchers WJG, van Kuppeveld FJM (2006a) Effects of picornavirus 3A proteins on protein transport and GBF1-dependent COP-I recruitment. *J Viol* **80:** 11852–11860

Wessels E, Duijsings D, Niu TK, Neumann S, Oorschot VM, de Lange F, Lanke KHW, Klumperman J, Henke A, Jackson CL, Melchers WJG, van Kuppeveld FJM (2006b) A viral protein that blocks Arf1-mediated COP-I recruitment by inhibiting the guanine nucleotide exchange factor GBF1. *Dev Cell* **11:** 191–201

Yamashita T, Kobayashi S, Sakae K, Nakata S, Chiba S, Ishihara Y, Isomura S (1991) Isolation of cytopathic small round viruses with BS-C-1 cells from patients with gastroenteritis. *J Infect Dis* **164:** 954–957

Yamashita T, Sakae K, Kobayashi S, Ishihara Y, Miyake T, Mubina A, Isomura S (1995) Isolation of cytopathic small round virus (Aichi virus) from Pakistani children and Japanese travelers from Southeast Asia. *Microbiol Immunol* **39:** 433–435

Yamashita T, Sakae K, Tsuzuki H, Suzuki Y, Ishikawa N, Takeda N, Miyamura T, Yamazaki S (1998) Complete nucleotide sequence and genetic organization of Aichi virus, a distinct member of the *Picornaviridae* associated with acute gastroenteritis in humans. *J Virol* **72:** 8408–8412

Yamashita T, Sugiyama M, Tsuzuki H, Sakae K, Suzuki Y, Miyazaki Y (2000) Application of a reverse transcription-PCR for identification and differentiation of Aichi virus, a new member of the Picornavirus family associated with gastroenteritis in humans. *J Clin Microbiol* **38:** 2955–2961

Yang S, Zhang W, Shen Q, Yang Z, Zhu J, Cui L, Hua X (2009) Aichi virus strains in children with gastroenteritis, China. *Emerg Infect Dis* **15:** 1703–1705

Zhou Y, Atkins JB, Rompani SB, Bancescu DL, Petersen PH, Tang H, Zou K, Stewart SB, Zhong W (2007) The mammalian Golgi regulates Numb signaling in asymmetric cell division by releasing ACBD3 during mitosis. *Cell* **129:** 163–178

Novel Human Adenovirus Strain, Bangladesh

Yuki Matsushima, Hideaki Shimizu, Atsuko Kano, Etsuko Nakajima, Yoko Ishimaru, Shuvra Kanti Dey, Yuki Watanabe, Fuyuka Adachi, Keiichiro Suzuki, Kohnosuke Mitani, Tsuguto Fujimoto, Tung Gia Phan, and Hiroshi Ushijima

We report a novel human adenovirus D (HAdV-65) isolated from feces of 4 children in Bangladesh who had acute gastroenteritis. Corresponding genes of HAdV-65 were related to a hexon gene of HAdV-10, penton base genes of HAdV-37 and HAdV-58, and a fiber gene of HAdV-9. This novel virus may be a serious threat to public health.

Human adenoviruses (HAdVs) are common pathogens that cause several diseases, such as pneumonia, acute gastroenteritis, and epidemic keratoconjunctivitis (*1*). HAdV infection is also associated with a serious adenovirus syndrome in immunocompromised patients after stem cell transplantation (*2*). Acute gastroenteritis causes illness and death in humans worldwide. Illness is associated with infection of enteric viruses, including rotavirus, astrovirus, norovirus, sapovirus, and adenovirus.

HAdVs are divided into 7 species (HAdV-A–G) on the basis of DNA genome homology. Most acute gastroenteritis related to HAdVs is caused by HAdV-F species (HAdV-40 and HAdV-41 (*3*,*4*). Recently, we detected HAdV-D in feces of children with diarrhea in Bangladesh (*5*). Other HAdV-D strains have also been associated with diarrhea in Kenya and Brazil (*6*,*7*).

We report a novel HAdV-D (HAdV-65) strain detected in feces of 4 children with acute gastroenteritis during October 2004–March 2005 in Bangladesh (*5*) and results of hexon, penton base, and fiber gene sequence analyses. We also report the full genome sequence of this virus, whose corresponding genes are closely related to the hexon gene of HAdV-10, penton base genes of HAdV-37 and HAdV-58, and the fiber gene of HAdV-9.

Author affiliations: Kawasaki City Institute of Public Health, Kanagawa, Japan (Y. Matsushima, H. Shimizu, A. Kano, E. Nakajima, Y. Ishimaru); Nihon University School of Medicine, Tokyo, Japan (K. Dey, H. Ushijima); Saitama Medical School, Saitama, Japan (Y. Watanabe, F. Adachi, K. Suzuki, K. Mitani); National Institute of Infectious Diseases, Tokyo (T. Fujimoto); and Blood Systems Research Institute, San Francisco, California, USA (T.G. Phan)

DOI: http://dx.doi.org/10.3201/eid1805.111584

The Study

Cloned virus (3 plaque purifications) was propagated in an A549 cell line, which was maintained in minimal essential medium supplemented with 1% fetal bovine serum (Cansera International Inc., Toronto, Ontario, Canada). Cultures were observed for 3–4 weeks for a cytopathic effect. After a cytopathic effect was observed, cell lysates were centrifuged at 1,430 × *g* for 20 min at 4°C. Supernatants were centrifuged at 72,000 × *g* for 3 h at 4°C. Pellets were resuspended in sterile water and treated with 10 μL (20 mg/mL) of proteinase K. DNA was extracted by using the phenol:chloroform:isoamyl alcohol (25:24:1) method (Invitrogen, Carlsbad, CA, USA) and precipitated with isopropyl alcohol.

PCR was performed in a total volume of 50 μL containing 20 pmol/μL of each primer, 2.5 mmol/L of dNTP, 1.25 units of GXL DNA polymerase (Takara, Shiga, Japan), and 5 μL of DNA template. After PCR products were purified by using the MinElute PCR Purification Kit (QIAGEN, Hilden, Germany), cycle sequencing was conducted by using the Genome Lab DTCS Quick Start Kit (Beckman Coulter Inc., Fullerton, CA, USA).

The complete genome of HAdV-65 was sequenced by using the primer walking method. The 5′ terminus of full-length DNA was phosphorylated with 20 units of T4 polynucleotide kinase and 0.5 μL of 100 mmol/L ATP, and ligated to a blunt *Eco*RI-*Not*I-*Bam*HI adaptor (1 pmol/μL) for 3 h at 8°C by using the DNA Ligation Mighty Mix Kit (Takara), PCRs with primer pairs containing adaptor sequences were conducted as described (*8*). DNA sequences were assembled by using the CEQ 2000XL DNA Analysis System version 4.3.9 (Beckman Coulter Inc.).

The genome of HAdV-65 was 35,172 bp. It had a GC content of 56.9%, and the inverted terminal repeat sequence of this virus was 150 bp. Phylogenetic trees were generated by using the maximum-likelihood method with MEGA5 (www.megasoftware.net) after alignment was performed by using ClustalW (www.clustal.org).

Complete genome analysis showed that HAdV-65 was ≥5.0% distant from any other HAdV-D reference strains (online Appendix Figure 1, panel A, wwwnc.cdc.gov/EID/article/18/5/11-1584-FA1.htm). On the basis of hypervariable loop 1 and loop 2, which encode the neutralization epitope of HAdVs, this virus clustered with HAdV-10 (online Appendix Figure 1, panels B and C). However, HAdV-65 was closely related to HAdV-37 and HAdV-58 in the hypervariable loop 1 and the Arg-Gly-Asp (RGD) loop of the penton base gene, respectively (online Appendix Figure 1, panels D and E). Phylogenetic analysis also showed that this novel virus clustered with HAdV-9 on the basis of the fiber gene sequence (online Appendix Figure 1, panel F). Sequences of HAdV-65 and 3 other strains (DC 11, 253, and 303) isolated from infants in this

study had identical hexon, penton base, and fiber genes.

Potential recombination in HAdV-65 was investigated by using the SimPlot program (http://sray.med.som.jhmi.edu/RaySoft/simplot_old/Version1/SimPlot_Doc_v13.html). DNA sequence alignments were created by using DNASIS Pro (Hitachi Solutions, Tokyo, Japan). SimPlot analysis showed no potential recombination in the hexon and fiber genes (online Appendix Figure 2, panels A and C, wwwnc.cdc.gov/EID/article/18/5/11-1584-FA2.htm), and recombination between the hypervariable loop 1 and the RGD loop was predicted in the penton base gene (online Appendix Figure 2, panel B). HAdV-65 had nucleotide identities of 97.9% to HAdV-10 in the hexon gene, 92.3% and 96.7% to HAdV-37 and HAdV-58, respectively, in the penton base gene, and 98.2% to HAdV-9 in the fiber gene. The GenBank accession number for HAdV-65 is AP012285.

Conclusions

We report the complete genome of HAdV-65, a novel human adenovirus isolated from children with gastroenteritis. Recombination is an essential feature for viral evolution and immune escape. Recombination can be facilitated by antiviral immune pressure and co-infection with different HAdV strains of the same species (*9*). Recently, newly identified HAdVs appeared to originate by recombination among ≥2 viruses. HAdV-53 was reported as a novel recombinant HAdV with a close genetic relationship to loop 1 and loop 2 of HAdV-22, the penton base gene of HAdV-37, and the fiber gene of HAdV-8. HAdV-56 had a loop 1 and loop 2 highly similar to those of HAdV-15 (*10*,*11*). All other regions of the genome were genetically related to HAdV-9.

HAdV-58 was recently characterized as a novel HAdV with unique hexon and fiber genes of HAdV-25 and HAdV-29 (*12*). In the present study, we demonstrated that hexon and fiber coding regions of HAdV-65 were formed by recombination in regions around these genes but not by potential recombination within these genes. The potential recombination site within the penton base gene is located at the central position between hypervariable loop 1 and the RGD loop.

These findings suggest that the most conserved sequences around the hexon and fiber genes and in the penton base gene may play a major role in recombination. In addition, this recombination mechanism may be more efficient in enabling new processes of infection and immune escape for maintaining HAdVs than individual small mutations, such as insertions, substitutions, and deletions.

Most recombinant HAdVs have been found in AIDS patients. (*9*,*13*). The RGD loop of the penton base protein can be digested by trypsin secreted in the intestines, which results in inhibition of proliferation of HAdV except for HAdV-F types in the intestines (*14*). In this study, HAdV-65 was isolated from infants who had lower immunocompetence and secretion rates of digestive enzymes than adults. These results indicate that emergence of HAdV-65 might have been caused by long coexistence of multiple HAdV-D types and depending on a decrease in immunity, as observed in AIDS patients, and decreased digestive capacity in the intestines.

We detected this type of recombination not only in HAdV-65, but also in 3 other HAdV strains that had a genome sequence identical with that of HAdV-65 from children in Bangladesh during 2004–2005. This finding indicates that this virus might be a newly emerging HAdV, which might be a serious threat to public health.

Acknowledgment

We thank Niwat Maneekarn for advice during the study.

This study was supported by grants-in-aid from the Ministry of Education and Sciences and the Ministry of Health, Labor and Welfare, Japan.

Mr Matsushima is a researcher at Kawasaki City Institute of Public Health, Kanagawa, Japan. His research interest is the epidemiology of viral infectious diseases in humans.

References

1. Benko M. Adenoviruses: pathogenesis. In: Mahy BW, van Regenmortel MH, editors. Encyclopedia of virology. 3rd ed. Oxford: Elsevier; 2008. p. 24–9.
2. Kampmann B, Cubitt D, Walls T, Naik P, Depala M, Samarasinghe S, et al. Improved outcome for children with disseminated adenoviral infection following allogeneic stem cell transplantation. Br J Haematol. 2005;130:595–603. http://dx.doi.org/10.1111/j.1365-2141.2005.05649.x
3. Akihara S, Phan TG, Nguyen TA, Hansman G, Okitsu S, Ushijima H, et al. Existence of multiple outbreaks of viral gastroenteritis among infants in a day care center in Japan. Arch Virol. 2005;150:2061–75. http://dx.doi.org/10.1007/s00705-005-0540-y
4. Shimizu H, Phan TG, Nisimura S, Okitsu S, Maneekarn N, Ushijima H, et al. An outbreak of adenovirus serotype 41 infection in infants and children with acute gastroenteritis in Maizuru City, Japan. Infect Genet Evol. 2007;7:279–84. http://dx.doi.org/10.1016/j.meegid.2006.11.005
5. Dey SK, Shimizu H, Phan TG, Hayakawa Y, Islam A, Salim AFM, et al. Molecular epidemiology of adenovirus infection among infants and children with acute gastroenteritis in Dhaka City, Bangladesh. Infect Genet Evol. 2009;9:518–22. http://dx.doi.org/10.1016/j.meegid.2009.02.001
6. Filho EP, da Costa Faria NR, Fialho AM, de Assis RS, Almeida MMS, Rocha M, et al. Adenoviruses associated with acute gastroenteritis in hospitalized and community children up to 5 years old in Rio de Janeiro and Salvador, Brazil. J Med Microbiol. 2007;56:313–9. http://dx.doi.org/10.1099/jmm.0.46685-0
7. Magwalivha M, Wolfaardt M, Kiulia NM, van Zyl WB, Mwenda JM, Taylor MB, et al. High prevalence of species D human adenoviruses in fecal specimens from urban Kenyan children with diarrhea. J Med Virol. 2010;82:77–84. http://dx.doi.org/10.1002/jmv.21673

8. Matsushima Y, Shimizu H, Phan TG, Ushijima H. Genomic characterization of a novel human adenovirus type 31 recombinant in the hexon gene. J Gen Virol. 2011;92:2770–5. http://dx.doi.org/10.1099/vir.0.034744-0
9. Robinson CM, Seto D, Jones MS, Dyer DW, Chodosh J. Molecular evolution of human species D adenoviruses. Infect Genet Evol. 2011;11:1208–17. http://dx.doi.org/10.1016/j.meegid.2011.04.031
10. Walsh MP, Chintakuntlawar A, Robinson CM, Madisch I, Harrach B, Hudson NR, et al. Evidence of molecular evolution driven by recombination events influencing tropism in a novel human adenovirus that causes epidemic keratoconjunctivitis. PLoS ONE. 2009;4:e5635–48. http://dx.doi.org/10.1371/journal.pone.0005635
11. Robinson CM, Singh G, Henquell C, Walsh MP, Peigue-Lafeuille H, Seto D, et al. Computational analysis and identification of an emergent human adenovirus pathogen implicated in a respiratory fatality. Virology. 2011;409:141–7. http://dx.doi.org/10.1016/j.virol.2010.10.020
12. Liu EB, Ferreyra L, Fischer SL, Pavan JV, Nates SV, Hudson NR, et al. Genetic analysis of a novel human adenovirus with a serologically unique hexon and a recombinant fiber gene. PLoS ONE. 2011;6:e24491–501. http://dx.doi.org/10.1371/journal.pone.0024491
13. Crawford-Miksza LK, Schnurr DP. Adenovirus serotype evolution is driven by illegitimate recombination in the hypervariable regions of the hexon protein. Virology. 1996;224:357–67. http://dx.doi.org/10.1006/viro.1996.0543
14. Albinsson B, Kidd AH. Adenovirus type 41 lacks an RGD αv-integrin binding motif on the penton base and undergoes delayed uptake in A549 cells. Virus Res. 1999;64:125–36. http://dx.doi.org/10.1016/S0168-1702(99)00087-8

Address for correspondence: Hiroshi Ushijima, Division of Microbiology, Department of Pathology and Microbiology, Nihon University School of Medicine, 30-1 Oyaguchi Kamicho, Itabashi-ku, Tokyo 173-8610, Japan; email: ushijima-hiroshi@jcom.home.ne.jp

collaborating in the diagnosis of pandemic influenza; Thais dos Santos and Mauricio Cerpa for revising the manuscript; and the US Centers for Disease Control and Prevention, the Chinese Centers for Disease Control (Beijing, China), and the Carlos III Institute (Madrid, Spain) for providing test kits and positive controls.

This study was supported in part by the Cuban National Program of Surveillance and Control for Acute Respiratory Infection of the Ministry of Health and the Pan American Health Organization.

Belsy Acosta, Alexander Piñón, Odalys Valdés, Clara Savón, Amely Arencibía, Elías Guilarte, Gonzalez Grehete, Suset Oropesa, Gonzalez Guelsys, Bárbara Hernández, Angel Goyenechea, Mayra Muné, Vivian Kouri, María G. Guzmán, and Alina Llop

Author affiliation: Instituto Pedro Kourí, Havana, Cuba

DOI: http://dx.doi.org/10.3201/eid1802.110547

References

1. Generic protocol influenza surveillance, PAHO-CDC [cited 2011 Mar 4]. http://www.paho.org/English/AD/DPC/CD/flu-snl-gpis.pdf
2. Panamerican Health Organization, World Health Organization. PAHO's director newsletter. Issue 7. April 26, 2009 [cited 2011 Mar 3]. http://www.paho.org/English/D/D_DNewsLetters_eng.asp
3. World Health Organization. WHO information for laboratory diagnosis of pandemic (H1N1) 2009 virus in humans [cited 2011 Mar 3]. http://www.who.int/csr/resources/publications/swineflu/diagnostic_recommendations/en/index.html
4. Coiras MT, Perez-Brena P, Garcia ML, Casas I. Simultaneous detection of influenza A, B, and C viruses, respiratory syncytial virus, and adenoviruses in clinical samples by multiplex reverse transcription nested-PCR assay. J Med Virol. 2003;69:132–44. http://dx.doi.org/10.1002/jmv.10255
5. Coiras MT, Aguilar JC, Garcia ML, Casas I, Perez-Brena P. Simultaneous detection of fourteen respiratory viruses in clinical specimens by two multiplex reverse transcription nested-PCR assays. J Med Virol. 2004;72:484–95. http://dx.doi.org/10.1002/jmv.20008
6. Pozo F, Garcia-Garcia ML, Calvo C, Cuesta I, Perez-Brena P, Casas I. High incidence of human bocavirus infection in children in Spain. J Clin Virol. 2007;40:224–8. http://dx.doi.org/10.1016/j.jcv.2007.08.010
7. López-Huertas MR, Casas I, Acosta-Herrera B, Garcia ML, Coiras MT, Perez-Brena P. Two RT-PCR based assays to detect human metapneumovirus in nasopharyngeal aspirates. J Virol Methods. 2005;129:1–7. http://dx.doi.org/10.1016/j.jviromet.2005.05.004
8. Valdés O, Piñón A, Acosta B, Savón C, González G, Arencibia A, et al. Design and implementation of a molecular method for influenza A virus (H1N1) in Cuba. Rev Cubana Med Trop. 2011;63:15–20.
9. Piñón A, Acosta B, Valdés O, Arencibia A, Savón C, González G, et al. Cuban strategy for the molecular characterization of the pandemic influenza A virus (H1N1). Rev Cubana Med Trop. 2011;63:21–9.
10. World Health Organization. CDC protocol of real-time RT-PCR for influenza A H1N1. April 28, 2009 [cited 2011 Mar 3]. http://www.who.int/csr/resources/publications/swineflu/CDCRealtimeRTPCR_SwineH1Assay-2009_20090430.pdf

Address for correspondence: Belsy Acosta, Instituto Pedro Kourí, Autopista Novia del Mediodía Km 6½, La Lisa, CP 17 100, Havana, Cuba; email: betsy@ipk.sld.cu

Letters

Letters commenting on recent articles as well as letters reporting cases, outbreaks, or original research are welcome. Letters commenting on articles should contain no more than 300 words and 5 references; they are more likely to be published if submitted within 4 weeks of the original article's publication. Letters reporting cases, outbreaks, or original research should contain no more than 800 words and 10 references. They may have 1 Figure or Table and should not be divided into sections. All letters should contain material not previously published and include a word count.

Hand, Foot, and Mouth Disease Caused by Coxsackievirus A6, Japan, 2011

To the Editor: Coxsackievirus A6 (CVA6) belongs to human enterovirus species A of the genus *Enterovirus*. According to a Japanese Infectious Agents Surveillance Report, this virus is one of the major causes of herpangina, an acute febrile disease characterized by vesicles, ulcers, and redness around the uvula, which occurs mainly in young children and infants. (*1*).

In June 2011, a sudden increase in cases of hand, foot, and mouth disease (HFMD) at pediatric sentinel sites (≈3,000 pediatric hospitals and clinics) was reported to the National Epidemiologic Surveillance of Infectious Diseases System in Japan. Compared with past numbers of cases over 30 years of surveillance, the number of cases of HFMD per sentinel site peaked in week 28 (July) of 2011 (10.97 cases per sentinel), particularly in western Japan (*2*). According to the Infectious Agents Surveillance Report (as of September, 18, 2011), CVA6 was detected in 709 HFMD cases and 156 herpangina cases throughout Japan (*1*).

Clinical samples (throat swab specimens and feces) obtained from sentinel sites in Shimane, Hyogo, Hiroshima, and Shizuoka, Japan, were screened for enteroviruses by using an enterovirus-specific reverse transcription PCR and sequence analysis of the partial viral protein (VP)4/VP2 or VP1 region (*3*). Among 93 clinical samples from 108 HFMD case-patients, we identified 74 case-patients as CVA6 positive by sequence analysis.

On the basis of sequence analysis of the entire VP1 region (GenBank accession nos. AB649286–AB649291), the consensus sequence

had 82.3%–82.5% nt identity (94.8%–95.4% aa identity) with the prototype CVA6 Gdula strain (GenBank accession no. AY421764). CVA6 was not isolated from clinical samples in a cell culture system. Therefore, most CVA6 strains were identified by molecular detection directly from clinical samples and sequence analysis. Some CVA6 strains were grown and isolated in suckling mice; these strains were antigenically identified as CVA6 by a neutralization test with specific antiserum against CVA6 (*4*).

In Japan, HFMD and herpangina are classified as category V infectious diseases. On the basis of clinical diagnosis, suspected infections were reported by pediatric sentinel sites on a weekly basis to the Infectious Disease Surveillance Center of the National Institute of Infectious Diseases (Tokyo, Japan). Typical clinical signs and symptoms of HFMD cases caused by CVA6 were fever, mild vesicles in oral mucosa, and skin blisters on hands, arms, feet, legs, buttocks, and nail matrixes (Figure). Some patients with HFMD had onychomadesis (periodic shedding of the nails) 1–2 months after onset of HFMD. Most cases of HFMD were self-limited. However, additional follow-up may be necessary for patients with onychomadesis who are treated at dermatology clinics.

As in other countries in the Asia–Pacific region, major causes of HFMD in Japan were CVA16 and enterovirus 71. In 2010, enterovirus 71 was identified as a major cause of HFMD (*1*). In contrast, CVA6 was consistently associated with herpangina, as were CVA2, CVA4, CVA5, and CVA10, but CVA6 was occasionally detected in HFMD case-patients. CVA6 was the major cause of herpangina in 2007, but an increase in the detection rate of CVA6 in HFMD case-patients was reported in Japan in 2009 (*1*).

HFMD outbreaks caused by CVA6 were reported in Singapore, Finland, and Taiwan in 2007–2009 (*5–8*). Recent HFMD outbreaks in Finland and Spain were associated with cases of onychomadesis 1–2 months after onset of HFMD (*6,8,9*). In Japan, cases of onychomadesis after onset of HFMD were reported in 2009 (*10*). Therefore, changes in clinical outcomes of CVA6-associated diseases should be investigated.

Although most HFMD cases caused by CVA6 in Japan were mild, CVA6 was also detected in other clinical samples, including cerebrospinal fluid from a patient with acute encephalitis in Hiroshima, which reaffirmed possible additional clinical manifestations during an HFMD outbreak caused by CVA6. Careful surveillance of disease and infectious agent activities are crucial in monitoring CVA6-associated HFMD, onychomadesis, and neurologic diseases. Nucleotide identity between CVA6 strains in Finland (2008) (*7*) and Japan (2011) was ≈95% in the partial VP1 region. More detailed genetic, phenotypic, and epidemiologic analyses of CVA6 are needed to determine the role of CVA6 in HFMD outbreaks with or without onychomadesis.

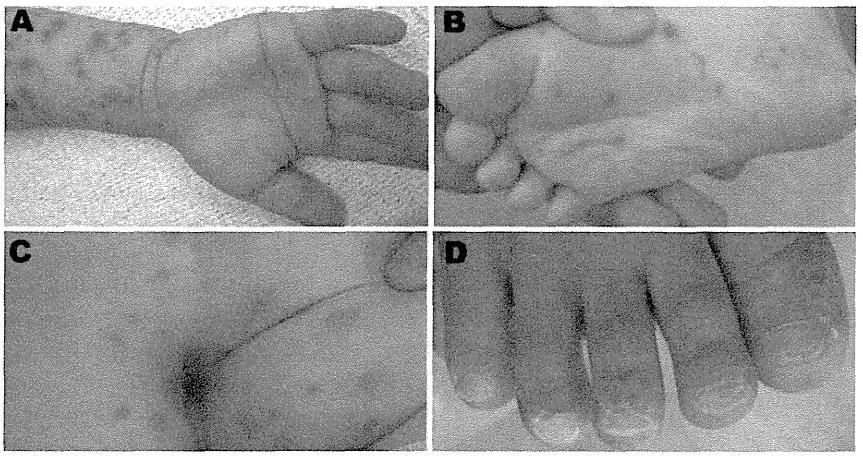

Figure. Typical clinical manifestations of hand, foot, and mouth disease associated with coxsackievirus CVA6 in Shizuoka, Japan, June–July, 2011. A) Hand and arm of a 2.5-year-old boy; B) foot and C) buttocks of a 6-year-old boy; D) nail matrix of a 20-month-old boy. A color version of this figure is available online (wwwnc.cdc.gov/EID/article/18/2/11-1147-F1.htm).

Acknowledgments

We thank the staff of prefectural and municipal public health institutes in Japan for virus detection, identification and molecular analysis, and Grant Hansman for critical review of the manuscript.

This study was supported in part by grants-in-aid for Scientific Research from the Ministry of Education, Culture, Sports, Science and Technology of Japan, and for research on emerging and re-emerging infectious diseases from the Ministry of Health, Labour and Welfare, Japan.

Tsuguto Fujimoto, Setsuko Iizuka, Miki Enomoto, Katsuhiko Abe, Kazuyo Yamashita, Nozomu Hanaoka, Nobuhiko Okabe, Hiromu Yoshida, Yoshinori Yasui, Masaaki Kobayashi, Yoshiki Fujii, Hiroko Tanaka, Miwako Yamamoto, and Hiroyuki Shimizu

Author affiliations: National Institute of Infectious Diseases, Tokyo, Japan (T. Fujimoto, K. Yamashita, N. Hanaoka, N. Okabe, H. Yoshida, Y. Yasui, H. Shimizu); Shimane Prefectural Institute of Public Health and Environmental Science, Shimane, Japan (S. Iizuka); Hyogo Prefectural Institute of Public Health and

Consumer Sciences, Hyogo, Japan (M. Enomoto); Hiroshima City Institute of Public Health, Hiroshima, Japan (K. Abe, Y. Fujii, H. Tanaka, M. Yamamoto); and Kobayashi Pediatric Clinic, Shizuoka, Japan (M. Kobayashi)

DOI: http://dx.doi.org/10.3201/eid1802.111147

References

1. Infectious Disease Surveillance Center. Virus isolation/detection from hand, foot and mouth disease cases, 2007–2011. Infectious Agents Surveillance Report [cited 2011 Nov 7]. http://idsc.nih.go.jp/iasr/prompt/s2graph-pke.html
2. Infectious Disease Surveillance Center. Infectious Disease Weekly Report, Hand-foot-mouth disease cases reported per sentinel weekly [cited 2011 Nov 7]. http://idsc.nih.go.jp/idwr/kanja/weeklygraph/06HFMD-e.html
3. Perera D, Shimizu H, Yoshida H, Tu PV, Ishiko H, McMinn PC, et al. A comparison of the VP1, VP2, and VP4 regions for molecular typing of human enteroviruses. J Med Virol. 2010;82:649–57.
4. Konno M, Yoshioka M, Sugie M, Maguchi T, Nakamura T, Kizawa M, et al. Fourteen years' surveillance of coxsackievirus group A in Kyoto 1996–2009 using mouse, RD-18S, and Vero cells. Jpn J Infect Dis. 2011;64:167–8.
5. Wu Y, Yeo A, Phoon MC, Tan EL, Poh CL, Quak SH, et al. The largest outbreak of hand; foot and mouth disease in Singapore in 2008: the role of enterovirus 71 and coxsackievirus A strains. Int J Infect Dis. 2010;14:e1076–81.
6. Österback R, Vuorinen T, Linna M, Susi P, Hyypia T. Waris M. Coxsackievirus A6 and hand, foot, and mouth disease, Finland. Emerg Infect Dis. 2009;15:1485–8.
7. Lo SH, Huang YC, Huang CG, Tsao KC, Li WC, Hsieh YC, et al. Clinical and epidemiologic features of coxsackievirus A6 infection in children in northern Taiwan between 2004 and 2009. J Microbiol Immunol Infect. 2011;44:252–7.
8. Blomqvist S, Klemola P, Kaijalainen S, Paananen A, Simonen ML, Vuorinen T, et al. Co-circulation of coxsackieviruses A6 and A10 in hand, foot and mouth disease outbreak in Finland. J Clin Virol. 2010;48:49–54.
9. Guimbao J, Rodrigo P, Alberto MJ, Omenaca M. Onychomadesis outbreak linked to hand, foot, and mouth disease, Spain, July 2008. Euro Surveill. 2010;15:19663.
10. Watanabe Y, Nanba C, Tohyama M, Machino H, Hashimoto K. Outbreak of nail matrix arrest following hand-foot-mouth disease [in Japanese]. Japanese Journal of Dermatology. 2011;121:863–7.

Address for correspondence: Hiroyuki Shimizu, Department of Virology II, National Institute of Infectious Diseases, Gakuen 4-7-1, Musashimurayama-shi, Tokyo 208-0011, Japan; email: hshimizu@nih.go.jp

Human and Porcine Hepatitis E Viruses, Southeastern Bolivia

To the Editor: Hepatitis E virus (HEV) genotypes 3 and 4 are considered to be primarily zoonotic (*1*). However, recent data indicate that both genotypes can be transmitted among humans through other routes (*2,3*). Observations of genetic distinctiveness between swine and human HEV strains circulating within the same region argue against exclusivity of zoonotic transmission (*4*). A recent report presented a remarkable example of such distinction between genotype 3 isolates in rural communities in southeastern Bolivia (*5*).

We examined HEV sequences obtained in that study to show the independent genetic origin of swine and human variants. Findings suggest disjunction between human and swine HEV strains in this epidemiologic setting, despite the potential for extensive cross-species exposure.

Using reference sequences from Lu et al. (*6*), we conducted subtype analysis of HEV open reading frame 2 sequences at nucleotide positions 826–1173 (GenBank accession no. AF060668) from isolates from 2 rural communities in southeastern Bolivia (*5*). Analysis showed that swine sequences belonged to subtype 3i and that the human sequences belonged to 3e.

We collected all available GenBank genotype 3 sequences covering this genomic region for which the dates of collection were documented. Sequences were used to estimate the time from the most recent common ancestor (tMRCA) by using BEAST version 1.6.1 (*7*). Estimated tMRCA for GenBank sequences was longer than for sequences from Bolivia alone (Table) or for all genotype 3 sequences together (Table).

To reduce the effect of close relatedness among human or swine HEV sequences from Bolivia on the tMRCA estimate, we used only 1 representative sequence per species from each community in the final analysis. This analysis identified an estimated tMRCA similar to that seen for GenBank sequences alone (Table, model F vs. model D). This estimate indicates that human and swine HEV isolates from southeastern Bolivia last shared a common ancestor ≈275 years ago (Table, model F). Thus, swine HEV strains from both rural communities belonged to subtype 3i, and the human HEV strains identified from the community of Bartolo, Bolivia, belonged to subtype 3e and shared an ancestor with swine strains almost 3 centuries ago.

This finding is surprising because the community of Bartolo has several potential risk factors for zoonotic transmission of HEV. There are ≈200 humans and ≈70 swine in Bartolo (*8*). Residents are mainly native Quechua and Guarani with some of mixed Spanish ancestry who subsist at a low socioeconomic level. Their main livelihood activities are agriculture and breeding of animals. Free-range pig farms are family owned. Because of its impoverished state, the community has no running water, and few houses have toilets. No facilities are suitable for safely slaughtering

Virus Genes (2012) 44:244–246
DOI 10.1007/s11262-011-0700-y

Detection and molecular characterization of cosavirus in adults with diarrhea, Thailand

Pattara Khamrin · Natthawan Chaimongkol · Rungnapa Malasao · Boonpa Suantai · Wilaiporn Saikhruang · Tipachan Kongsricharoern · Nuthapong Ukarapol · Shoko Okitsu · Hiroyuki Shimizu · Satoshi Hayakawa · Hiroshi Ushijima · Niwat Maneekarn

Received: 30 August 2011 / Accepted: 5 December 2011 / Published online: 16 December 2011

Abstract Human cosavirus (HCoSV) is a newly discovered virus in *Picornaviridae* family. At present it is not clear whether HCoSV is associated with diseases, including gastroenteritis in humans, as epidemiological data is limited. Epidemiological surveillance of HCoSV was conducted on 150 fecal specimens collected from children and 150 samples from adults with diarrhea in Thailand by RT-PCR screening. HCoSV was found in a single adult specimen and not in any of the fecal specimens from children. This represents the first report of HCoSV infection in patients with diarrhea in Thailand. Extensive epidemiological surveillance of novel viruses associated with diarrhea in other populations may provide a better understanding of the distribution, genetic diversity, and association of the viral agents associated with acute gastroenteritis in humans.

Keywords Cosavirus · Diarrhea · Thailand

P. Khamrin · N. Chaimongkol · R. Malasao · B. Suantai · W. Saikhruang · N. Maneekarn (✉)
Department of Microbiology, Faculty of Medicine, Chiang Mai University, 110 Intawarorose, Sriphoom, Muang, Chiang Mai 50200, Thailand
e-mail: nmaneeka@med.cmu.ac.th

T. Kongsricharoern
Pediatric Hematology Unit, Nakornping Hospital, Chiang Mai, Thailand

N. Ukarapol
Department of Pediatrics, Faculty of Medicine, Chiang Mai University, Chiang Mai, Thailand

S. Okitsu · S. Hayakawa · H. Ushijima
Division of Microbiology, Department of Pathology and Microbiology, Nihon University School of Medicine, Tokyo, Japan

H. Shimizu
Department of Virology II, National Institute of Infectious Diseases, Tokyo, Japan

Acute gastroenteritis is one of the most common diseases in children and adults, and continues to be a significant cause of morbidity and mortality worldwide [1]. Most recently, several viruses related to diarrhea have been discovered in human stool samples, mostly by viral metagenomic strategy [2]. Once new viruses related to diarrheal diseases are discovered, there is a need to constantly monitor the prevalence of these viruses in the community for clarification of their clinical significance. Human cosavirus (HCoSV), a new member in *Picornaviridae*, was originally identified from stool samples of both healthy children and non-polio acute flaccid paralysis patients in Pakistan and Afghanistan [3]. In addition, a stool sample from a 64-year-old woman collected in Scotland was positive for HCoSV by RT-PCR [3]. A report from the United States demonstrated that HCoSV was also detected in untreated sewage samples collected from multiple cities [4]. In addition, a novel candidate species of HCoSV (HCoSV-E1) was identified in the stool sample of a child suffering from diarrhea in Australia [5]. In China, HCoSV was reported recently from healthy and diarrheic children [6]. The HCoSV genome is about 7.6 kb long and has the typical picornavirus genome organization, but its genomic organization lacks a leader (L) sequence. The genome consists of four structural viral proteins (VP4, VP2, VP3, VP1), and nine nonstructural proteins (2A1, 2A2, 2B, 2C, 3A, 3B1, 3B2, 3C, and 3D) [3]. HCoSV presently comprises of one proposed species (A) and four candidate species (B–E), and further subdivided into at least eight genotypes (A1–A4, B1, C1, D1, E1)

[3, 5]. Although HCoSV is geographically widespread, the pathogenicity and the association with diseases in humans are currently unknown. Here, we report the detection of HCoSV in adults with diarrhea in Thailand.

A total of 150 stool samples were collected from children hospitalized with diarrhea and other 150 stool samples were collected from adult patients with diarrhea during January to December, 2008, in Chiang Mai, Thailand. The study was conducted with the approval of the ethical committee for human rights related to human experimentation, Faculty of Medicine, Chiang Mai University (No. 181/2554). The viral genome was first extracted from 10% fecal suspension supernatant using the QIAamp viral RNA Mini Kit (Qiagen, Germany). The presence of HCoSV was detected by RT-nested PCR which targeted the 5′ untranslated region (UTR) and specifically generated a PCR amplicon of 316 bp [3]. The amplified gene of HCoSV was subjected to a direct sequencing using BigDye Terminator Cycle Sequencing Kit (Applied Biosystems, Foster City, CA). The sequence was compared with those of reference strains available in the NCBI GenBank database using BLAST server (www.ncbi.nlm.nih.gov/blast). Phylogenetic and molecular evolutionary analyses were conducted using MEGA 4 [7]. The nucleotide sequence of HCoSV strain described in the present study was deposited in the GenBank under accession number JF749990.

HCoSV, designated CMHA172/2008 was found in one of 150 specimens collected from adults with diarrhea, while all samples from children were negative. The HCoSV strain CMHA172/2008 found in an adult with diarrhea had a pairwise nucleotide sequence identity ranging from 93.6 to 95.4% with HCoSV-D strains FL2-6-C5, 5004, 0961, and FL2-7-C9, across the partial 5′ UTR region characterized. Comparison of the 5′ UTR sequence of CMHA172/2008 and other HCoSV prototype strains (0553 HCoSV-A1, 2263 HCoSV-B1, 5152 HCoSV-C1, 5004 HCoSV-D1), revealed the highest nucleotide sequence identity to 5004 HCoSV-D1 at 95.4%, while the other prototype strains of 0553 HCoSV-A1, 2263 HCoSV-B1, and 5152 HCoSV-C1, sequence identities ranged from

Table 1 Partial 5′ UTR nucleotide sequence identities between the sequences of HCoV found in this study and HCoV reference strains

HCoV strains	Nucleotide sequence identity (%)				
	CMHA172/08	0553 HCoSV-A1	2263 HCoSV-B1	5152 HCoSV-C1	5004 HCoSV-D1
CMHA172/08	100.0				
0553 HCoSV-A1	83.1	100.0			
2263 HCoSV-B1	82.3	76.4	100.0		
5152 HCoSV-C1	87.7	84.0	80.0	100.0	
5004 HCoSV-D1	**95.4**	81.3	83.7	85.0	100.0

The highest nucleotide sequence identity between the HCoSV strain detected in the present study and the reference strain 5004 HCoSV-D1 is presented in boldface

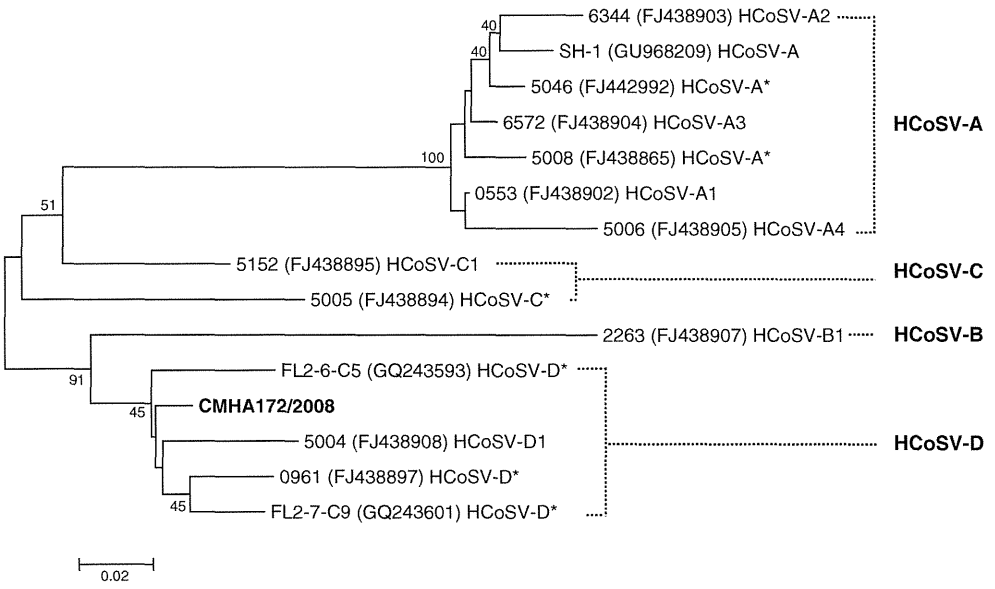

Fig. 1 Phylogenetic analysis of the partial nucleotide sequence encoding the 5′ UTR region of HCoSVs. The tree was generated using the neighbor-joining algorithm, in MEGA 4 [7]. Scale bar indicates nucleotide substitutions per site and bootstrap values (>40) are indicated for the corresponding nodes, based on a resampling analysis of 1,000 replicates. The HCoSV strain detected in the present study is presented in boldface

82.3 to 87.7% (Table 1). The phylogenetic analysis (Fig. 1) indicates that CMHA172/2008 belongs to HCoSV-D, clustering with other reference strains of HCoSV-D with 45% bootstrap value support. Although bootstrap support value was low, the virus has been assigned on the basis of the high level of nucleotide sequence identity (Table 1).

From literature search, there was no report of HCoSV from diarrheic patients in Thailand. One case of HCoSV found in this study was from an adult with diarrhea and the virus belonged to the HCoSV-D. Since the detection rate of this virus in stool specimens is relatively low and the study was not performed on healthy individuals, the relationship of this viral agent with diarrhea in human is still unclear. Previously, the intensive epidemiological surveillances of diarrheal viruses in Chiang Mai, Thailand have focused on group A rotavirus and calicivirus, which are the main causative agents for acute gastroenteritis in the area [8, 9]. However, more than half of the fecal specimens collected from diarrheic patients were negative for the screened viruses. Therefore, further extensive epidemiological surveillance with larger numbers of clinical specimens and screen for other types of viruses are necessary and may provide a better understanding of the distribution, genetic diversity, and association of the viral agents with acute gastroenteritis in humans. In addition, to further obtain the information of HCoSV infections, seroprevalence studies may help to estimate anti-HCoSV antibody prevalence in human populations.

Acknowledgments This research was supported by a grant for Medical Research, Faculty of Medicine, Chiang Mai University, Thailand.

References

1. D.M. Musher, B.L. Musher, N. Engl. J. Med. **351**, 2417–2427 (2004)
2. S.R. Finkbeiner, A.F. Allred, P.I. Tarr, E.J. Klein, C.D. Kirkwood, D. Wang, PLoS Pathog. **4**, e1000011 (2008)
3. A. Kapoor, J. Victoria, P. Simmonds, E. Slikas, T. Chieochansin, A. Naeem, S. Shaukat, S. Sharif, M.M. Alam, M. Angez, C. Wang, R.W. Shafer, S. Zaidi, E. Delwart, Proc. Natl. Acad. Sci. USA **105**, 20482–20487 (2008)
4. O. Blinkova, K. Rosario, L. Li, A. Kapoor, B. Slikas, F. Bernardin, M. Breitbart, E. Delwart, J. Clin. Microbiol. **47**, 3507–3513 (2009)
5. L.R. Holtz, S.R. Finkbeiner, C.D. Kirkwood, D. Wang, Virol. J. **5**, 159 (2008)
6. X.Q. Dai, X.G. Hua, T.L. Shan, E. Delwart, W. Zhao, J. Clin. Virol. **48**, 228–229 (2010)
7. K. Tamura, J. Dudley, M. Nei, S. Kumar, Mol. Biol. Evol. **24**, 1596–1599 (2007)
8. P. Khamrin, N. Maneekarn, A. Thongprachum, N. Chaimongkol, S. Okitsu, H. Ushijima, J. Med. Virol. **82**, 289–296 (2010)
9. P. Khamrin, N. Maneekarn, R. Malasao, T.A. Nguyen, S. Ishida, S. Okitsu, H. Ushijima, Infect. Genet. Evol. **10**, 467–472 (2010)

JVI
Journals.ASM.org

Valosin-Containing Protein (VCP/p97) Is Required for Poliovirus Replication and Is Involved in Cellular Protein Secretion Pathway in Poliovirus Infection

Minetaro Arita, Takaji Wakita, and Hiroyuki Shimizu

Department of Virology II, National Institute of Infectious Diseases, Musashimurayama-shi, Tokyo, Japan

Poliovirus (PV) modifies membrane-trafficking machinery in host cells for its viral RNA replication. To date, ARF1, ACBD3, BIG1/BIG2, GBF1, RTN3, and PI4KB have been identified as host factors of enterovirus (EV), including PV, involved in membrane traffic. In this study, we performed small interfering RNA (siRNA) screening targeting membrane-trafficking genes for host factors required for PV replication. We identified valosin-containing protein (VCP/p97) as a host factor of PV replication required after viral protein synthesis, and its ATPase activity was essential for PV replication. VCP colocalized with viral proteins 2BC/2C and 3AB/3B in PV-infected cells and showed an interaction with 2BC and 3AB but not with 2C and 3A. Knockdown of VCP did not suppress the replication of coxsackievirus B3 or Aichi virus. A VCP-knockdown-resistant PV mutant had an A4881G (a mutation of E253G in 2C) mutation, which is known as a determinant of a secretion inhibition-negative phenotype. However, knockdown of VCP did not affect the inhibition of cellular protein secretion caused by overexpression of each individual viral protein. These results suggested that VCP is a host factor required for viral RNA replication of PV among membrane-trafficking proteins and provides a novel link between cellular protein secretion and viral RNA replication.

Poliovirus (PV) is a small nonenveloped virus with a single-strand positive genomic RNA of about 7,500 nucleotides (nt) belonging to *Human enterovirus C* in the genus *Enterovirus*, the family *Picornaviridae*. PV is the causative agent of poliomyelitis, which is caused by the destruction of motor neurons by the direct infection of PV in the cells (17, 26). With established live attenuated oral PV vaccine (OPV) and inactivated PV vaccine (IPV) for PV (72, 73), the global eradication program for poliomyelitis has been continued by the Global Polio Eradication Initiative (GPEI) of the World Health Organization (WHO) since 1988. In the eradication program for poliomyelitis, antivirals for PV are anticipated to have some roles in the posteradication era of PV (24, 25) although currently there is no antiviral available for therapeutic use for PV infection.

Antiviral candidates have served as useful tools for the study of PV infection in addition to their potential use in therapy. Antivirals for PV have been identified at every stage of PV infection, including binding to cells, uncoating, protein synthesis, RNA replication, and encapsidation (reviewed in references 9, 21, and 70). As viral RNA replication inhibitors, guanidine hydrochloride (GuHCl), brefeldin A (BFA), and PIK93 are well characterized in terms of the target and the mechanism of inhibition and also represent predominant groups of replication inhibitor. GuHCl targets viral 2C and/or 2BC proteins along with some benzimidazole derivatives (30, 35, 77) and inhibits initiation of negative-strand RNA synthesis (10, 16, 20). BFA is an inhibitor of BFA-sensitive guanine nucleotide exchange factors (GEFs) and suppresses activation of ADP ribosylation factors (Arfs) by stabilizing a transitional inactive complex, the Arf-GDP-Sec7 domain of GEFs (66). BFA inhibits replication of enterovirus (EV) including PV by targeting GBF1 (11, 27, 44, 60, 91). The inhibitory effect of BFA is limited in EV replication and not conserved in general picornavirus replication (e.g., replication of encephalomyocarditis virus [EMCV] is insensitive for BFA) (44). Other GEFs, BIG1/BIG2, are also required for EV replication via direct and indirect interaction with viral 3A and 3CD proteins (12, 91). PIK93, a phosphatidylinositol 4-kinase III beta (PI4KB) inhibitor, has been identified to act as an antienterovirus compound (43). PIK93 inhibits PI4KB activity to suppress interaction of phosphatidylinositol-4-phosphate with viral 3D polymerase on the reorganized membrane vesicles (43). Recent analyses of picornavirus 3A proteins suggest an important role of ACBD3, which is a Golgi protein interacting with giantin (80) to form a PI4KB/ACBD3/3A protein complex for viral replication (37, 75). Interestingly, PIK93 belongs to a group of anti-PV compounds in terms of a resistance mutation of PV (G5318A [A70T mutation in 3A]) that confers resistance to enviroxime (3). Enviroxime is an antipicornavirus compound that inhibits positive-strand RNA synthesis by preventing normal formation of replication complex (18, 40, 93). To date, several anti-PV compounds have been identified in this group as enviroxime-like compounds (3, 5–7, 31). One of the enviroxime-like compounds, the PI4KB-specific inhibitor T-00127-HEV1, targets PI4KB activity for its anti-PV activity but does not have anti-hepatitis C virus (HCV) activity, suggesting that PI4KB is a target of enviroxime-like compounds in picornavirus replication (3). An antipicornavirus compound, Ro-09-0179, targets the Golgi apparatus as well as BFA (47, 74), underscoring the importance of the membrane-trafficking pathway not only for PV replication but also as a target pathway for an antiviral drug.

The membrane-trafficking pathway provides general targets, including Rab and Arf families, for replication of bacteria and

Received 17 January 2012 Accepted 23 February 2012
Published ahead of print 29 February 2012
Address correspondence to Minetaro Arita, minetaro@nih.go.jp.
Supplemental material for this article may be found at http://jvi.asm.org/.

doi:10.1128/JVI.00114-12

viruses (reviewed in reference 67). In PV replication, ARF1, ACBD3, GBF1, BIG1/2, RTN3, and PI4KB are involved in the membrane trafficking pathway (12, 37, 43, 75, 83, 91). In PV infection, the membrane traffic pathway is utilized for the formation of the replication complex and for nonlytic virus release from the infected cells (48, 84). Viral proteins 3A and 2BC are involved in formation of vesicles similar to that observed in PV-infected cells (82) and in inhibition of cellular protein secretion (34). The inhibitory effect of 3A on cellular protein secretion is not generally conserved in picornavirus (23) but might be compensated by other viral proteins (e.g., 2BC protein for foot-and-mouth disease virus infection) (62). Cellular protein secretion is inhibited during PV infection (34); however, PV mutants that did not inhibit cellular protein secretion have been isolated and did not show a significant growth defect (15, 19, 32). Therefore, the importance of cellular protein secretion in picornavirus infection as well as the responsible host factors remained to be elucidated.

In the present study, we have performed a screening with a library of small interfering RNAs (siRNAs) targeting membrane-trafficking genes to identify host factors involved in PV replication. We identified valosin-containing protein (VCP) as a novel host factor for PV replication. VCP is a cellular ATPase that belongs to the class I AAA+ (ATPase associated with diverse cellular activities) family (92) and has roles in a variety of cellular processes. We found that ATPase activity of VCP is essential for PV replication and that viral proteins 2BC and 3AB interact with VCP. Knockdown of VCP did not suppress the replication of coxsackievirus B3 (CVB3), which is a member of another EV species, *Human enterovirus B*, or of Aichi virus (AV), which is a member of another genus, *Kobuvirus*, of the family *Picornaviridae*. A PV-resistant mutant that showed improved growth in VCP-knockdown cells contained the mutation A4881G (E253G in 2C [2C-E253G]), which is known as the determinant of a secretion inhibition-negative phenotype of a PV mutant (19). However, knockdown of VCP did not suppress the inhibition of cellular protein secretion caused by overexpression of viral proteins 2B, 2BC, 3A, and 3AB. These results suggested that VCP is a host factor required for viral RNA replication of PV among membrane-trafficking proteins and provides a novel link between cellular protein secretion and viral RNA replication.

MATERIALS AND METHODS

Cells, viruses, plasmids, antibodies, and siRNA library. RD cells (human rhabdomyosarcoma cell line) and HEK293 cells (human embryonic kidney cells) were cultured as monolayers in Dulbecco's modified Eagle medium (DMEM) supplemented with 10% fetal calf serum (FCS). RD cells were used for titration of virus and characterization of eeyarestatin I (EerI). HEK293 cells were used for siRNA screening to identify host factors of PV replication. PV pseudovirus (TE-PV-Fluc mc), which encapsidated a luciferase-encoding PV replicon with capsid proteins derived from PV1 (Mahoney), was used for siRNA screening according to the condition established for antienterovirus compound screening (1, 4, 7). Expression vectors for Flag-tagged and enhanced green fluorescent protein (EGFP)-fused VCP mutants [wild-type (wt) VCP, VCP(K524A), VCP(R191Q), and VCP(A232E), constructed based on mouse VCP sequence that has 100% amino acid similarity to human VCP; mutated residues are indicated in parentheses] were kind gifts from Akira Kakizuka (Laboratory of Functional Biology, Kyoto University Graduate School of Biostudies, Japan) (59). A cDNA clone of an Aichi virus replicon was a generous gift from Jun Sasaki (Department of Virology and Parasitology, Fujita Health School of Medicine) (63). EGFP fusions of VCPs with FLAG tags on their C termini were used for immunoprecipitation. Antibodies against PV 3A and 3B were raised in rabbits with peptides CDLLQAVDS QEVRDY (amino acids [aa] 23 to 36 of PV 3A protein) and CNKKPNV PTIRTAKVQ (amino acids 8 to 22 of PV 3B protein), respectively. Expression vectors for PV proteins (2B, 2BC, 2C, 3A, and 3AB) were constructed with pKS435, where expression of viral proteins was controlled under the HEF-1α promoter (4). 3AB mutant proteins used in this study are as follows: wild-type 3AB, 3AB-His (3AB protein with a six-histidine tag), wild-type 3A, 3AB protein lacking amino acids 61 to 87 of 3A protein [3A(Δ61–87)B], and 3AB protein lacking amino acids 1 to 41 of 3A protein [3A(Δ1–41)B]. An siRNA library targeting human membrane-trafficking genes (total, 140 genes) was purchased from Thermo-Fisher Scientific as a form of siGENOME Smart pools, which contain four sets of different siRNAs for each mRNA and were validated of over 75% knockdown efficiency of target mRNAs. As control siRNAs, siGLO Cyclophilin B control siRNA, siGLO Lamin A/C control siRNA, siGENOME Nontargeting siRNA 1 and 2, siGENOME RISC-Free control siRNA, and siGENOME Tox transfection control were used in each experiment. EerI was purchased from Santa Cruz Biotechnology, Inc.

siRNA screening. Duplex RNA of each siRNA (at a final concentration of 50 nM) was transfected into HEK293 cells (5.0×10^3 cells in 100 μl medium per well) in 96-well plates (White Opaque Tissue Culture Plate, Becton Dickinson) by using DharmaFECT1 transfection reagent (Thermo Fisher Scientific) according to the manufacturer's instructions. The cells were incubated at 37°C for 72 h and then subjected to PV pseudovirus infection. Transfection efficiency of siRNA in the cells was evaluated by the efficiency of incorporation of fluorescence-labeled siRNA (siGLO control siRNAs) in the transfected cells at 24 h posttransfection (p.t.) and by the efficiency of cell death in the cells transfected with the siGENOME Tox transfection control at 96 h p.t. (Cells transfected with this control reagent die by apoptosis.) For analysis of expression levels of target proteins in siRNA-transfected cells, cell lysates of siRNA-transfected cells in a well of 24-well plates were prepared at 72 h p.t. in 100 μl of cell lysis buffer (21 mM HEPES buffer [pH 7.4], 1.8 mM disodium hydrogen phosphate, 137 mM NaCl, 4.8 mM KCl, 0.5% Nonidet P-40, and 5 mM EDTA, supplemented with a Complete Mini protease inhibitor cocktail tablet [Roche]) and then subjected to Western blot analysis.

At 72 h p.t., siRNA-transfected cells were inoculated with 800 IU of PV pseudovirus in a total of 200 μl per well at 96 h p.t. of siRNAs. The cells were incubated at 37°C for 7 h, and then the luciferase activity in the cells was measured with a Steady-Glo Luciferase Assay System (Promega) using a 2030 ARVO X luminometer (PerkinElmer) according to the manufacturer's instructions. The mean number of net relative light units (RLU) detected in mock-treated cells was around 1.4×10^4 RLU, with standard deviations of 15% of the mean. PV pseudovirus infection in siRNA-transfected cells was calculated as a percentage of luciferase activity of the infected cells, where the luciferase activity in mock-transfected cells in the absence of compounds was taken as 100%. To evaluate the direct effect of siRNA treatment, net PV pseudovirus infection, which is a ratio of percent PV pseudovirus infection in siRNA-transfected cells to percent cell viability, was determined for each siRNA treatment. Net PV pseudovirus infection in mock-transfected cells was 1.

Rescue of PV replication in VCP-knockdown cells by mutant VCP expression. HEK293 cells transfected with siRNA targeting VCP (VCP-siRNA) or mock-transfected cells were transfected with expression vectors encoding EGFP-fused VCP mutants derived from mouse VCP (59) or EGFP (control) by using a Lipofectamine 2000 reagent (Invitrogen) at 48 h after siRNA transfection. Cells were incubated at 37°C for 24 h after DNA transfection. RNA transcripts of the PV replicon were obtained by using a RiboMAX Large-Scale RNA Production System-T7 kit (Promega) with DraI-linearized DNA of pPV-Fluc mc, which encodes a PV replicon based on PV1 (Mahoney) with a firefly luciferase gene instead of the capsid-coding region, as the template. RNA transcripts were transfected into the cells by using a Lipofectamine RNAiMAX reagent (Invitrogen). Cells were harvested at 7 h p.t. of the RNA transcripts, and then luciferase activity in the cells was measured with a Steady-Glo Luciferase Assay Sys-